ITUPublications

International Telecommunication Union
Radiocommunication Sector

Report ITU-R RA.2552-0

(03/2025)

RA Series: Radio astronomy

Methodology for the coordination of International Mobile Telecommunications systems and stations of the radio astronomy service operating in the frequency band 42.5-43.5 GHz

Foreword

The role of the Radiocommunication Sector is to ensure the rational, equitable, efficient and economical use of the radio-frequency spectrum by all radiocommunication services, including satellite services, and carry out studies without limit of frequency range on the basis of which Recommendations are adopted.

The regulatory and policy functions of the Radiocommunication Sector are performed by World and Regional Radiocommunication Conferences and Radiocommunication Assemblies supported by Study Groups.

Policy on Intellectual Property Right (IPR)

ITU-R policy on IPR is described in the Common Patent Policy for ITU-T/ITU-R/ISO/IEC referenced in Resolution ITU-R 1. Forms to be used for the submission of patent statements and licensing declarations by patent holders are available from https://www.itu.int/ITU-R/go/patents/en where the Guidelines for Implementation of the Common Patent Policy for ITU-T/ITU-R/ISO/IEC and the ITU-R patent information database can also be found.

Series of ITU-R Reports

(Also available online at https://www.itu.int/publ/R-REP/en)

Series	Title
BO	Satellite delivery
BR	Recording for production, archival and play-out; film for television
BS	Broadcasting service (sound)
BT	Broadcasting service (television)
F	Fixed service
M	Mobile, radiodetermination, amateur and related satellite services
P	Radiowave propagation
RA	**Radio astronomy**
RS	Remote sensing systems
S	Fixed-satellite service
SA	Space applications and meteorology
SF	Frequency sharing and coordination between fixed-satellite and fixed service systems
SM	Spectrum management
TF	Time signals and frequency standards emissions

***Note**: This ITU-R Report was approved in English by the Study Group under the procedure detailed in Resolution ITU-R 1.*

Electronic Publication
Geneva, 2025

REPORT ITU-R RA.2552-0

Methodology for the coordination of International Mobile Telecommunications systems and stations of the radio astronomy service operating in the frequency band 42.5-43.5 GHz

(2025)

TABLE OF CONTENTS

Page

1 Introduction and background

The radio astronomy service (RAS) makes extensive use of the frequency band 42.5-43.5 GHz for spectral line observations of compound silicon monoxide (SiO) and for continuum observations. As with many science uses of the spectrum, RAS must go where the physics leads, and the use of other frequencies for spectral line observations of the SiO molecule is not possible (see Fig. 1; a spectrum from the Kleinmann-Low Nebula in the centre of the famous Orion Nebula showing emission from SiO and other molecules[1]). Recommendation ITU-R RA.314 provides further information about preferred frequency bands for RAS.

The purpose of this Report is twofold: 1) to provide guidance to administrations regarding determining whether a compatibility issue exists between International Mobile Telecommunications (IMT) systems operating in the mobile service allocation 37-43.5 GHz and RAS stations operating in 42.5-43.5 GHz; and 2) to develop guidance for enhancement of coexistence.

RAS observatories that make use of this frequency range are found in all three ITU regions and in multiple administrations around the world. Many of these observatories are located at remote sites; however, control of the radiation environment, as well as propagation conditions, varies from site to site. In many cases, geographic separation using existing quiet zones established for the protection of RAS may be sufficient (see Report ITU-R RA.2259 for more details on existing quiet zones worldwide).

FIGURE 1

Radio astronomy observations in the centre of the Orion Nebula from 42.5-45 GHz

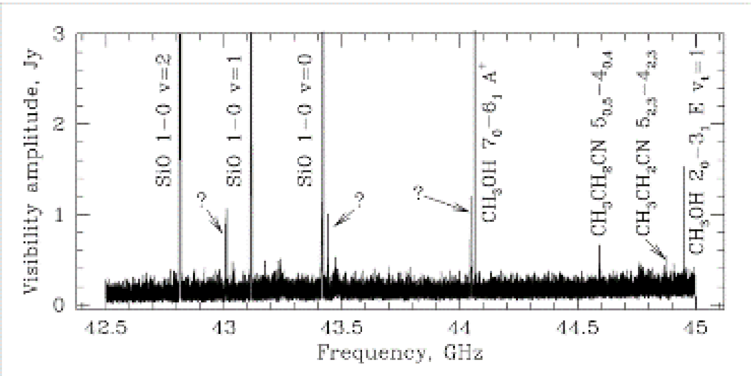

The Radio Regulations (RR) provide relevant information to administrations regarding the operation of RAS systems and minimizing impacts from active services (RR Nos **29.8** to **29.13**).

2 Technical characteristics

2.1 RAS protection criteria

Protection criteria for RAS systems in this frequency band are detailed in the most recent version of Recommendation ITU-R RA.769 and reproduced in Table 1 below. Criteria for broadband (continuum) observations are, by necessity, different than those for narrow-band (spectral line) operation. There are less stringent protection criteria for very long baseline interferometry (VLBI) stations (which includes all of the very long baseline array stations); these threshold interference

---

[1] G. G. Moorey *et al.*, "Cryogenically Cooled Millimetre-Wave Front Ends for the Australia Telescope," 2008 38th European Microwave Conference, Amsterdam, 2008, pp. 155-158.

levels are listed in Table 3 of Recommendation ITU-R RA.769. This is because very long baselines make VLBI stations less susceptible to harmful interference. For calculation of coordination distances, the limit appropriate to a given station should be used. It is noted, however, that VLBI stations need to perform calibration measurements from time to time, which are usually carried out in the continuum observing mode.

TABLE 1

Technical/operational characteristics of RAS stations

Characteristic	Details
Protection criterion *I*/*N* (dBW)	Spectral line observations: −207, 500 kHz bw; continuum: −191, 1 GHz bw; VLBI: −139, 1 GHz bw (Rec. ITU-R RA.769)
Characteristics of RAS stations	Recommendation ITU-R RA.769 assumes that the interference enters the antenna through the 0 dBi side-lobe, and hence the gain is assumed to be isotropic. If the antenna pattern for the RAS is needed, it can be obtained via Rec. ITU-R SA.509.

2.2 Sample IMT systems characteristics for use in calculation of coordination distances

Typical IMT-2020 characteristics between 24.25 GHz and 86 GHz are provided in ITU-R Document 5-1/36, Attachment 2, hereafter referred to as IMT.PARAMETER. Technical and operational characteristics based on national licensing decisions should be used when available, in addition to any characteristics of the actual planned deployment. The power control method of IMT user equipment (UE), which dynamically varies the UE transmit power based on the current link budget between UE and its host base station (BS), is described in Recommendation ITU-R M.2101, section 5. Channel models to be used in the calculation of the link budget for power control are provided by 3GPP TR 38.901 sections 7.2 and 7.4.1. Furthermore, the antenna gains of both stations, BS and UE, must be considered for calculation of the link budget for each instance of time and each particular device (antenna directions, and thus gains, are time-dependent for active antenna systems (AAS)).

3 Elements to be considered for coordination

The coordination process between RAS sites and IMT deployments depends upon several factors and should be evaluated on a case-by-case basis. In assessing compatibility, deployment of IMT systems near existing RAS sites should account for the need to protect extremely sensitive RAS systems from interference.

The implementation of new IMT deployments near RAS sites may be done through the use of coordination distances, calculated using aggregate deployment models and propagation conditions for the site in question. Siting of systems closer than the calculated distances should be carried out through case-by-case coordination, in which further analysis, considerations, and mitigation techniques may be employed.

3.1 Determination of coordination distances

The means to calculate the aggregate signal at a given site from proposed IMT deployments, and thus to determine coordination distances based on the protection criteria given in Recommendation ITU-R RA.769 and the data loss provisions of Recommendation ITU-R RA.1513, involve several factors and steps. Analysis methodology for determination of signals from IMT systems is provided in Recommendation ITU-R M.2101, and is based on Monte Carlo simulations of specified IMT BS deployments with randomly located UE serviced by the BSs. A given percentage of devices are defined as transmitting during any given simulation, with a range of transmitter power potentially subject to power control, and both the UE and the BSs incorporate AAS with main beams that dynamically track UE. As the transmission follows a Time-Division Duplex (TDD) scheme, the BS beams will point towards each user device subsequently, and, using specified calculated antenna patterns, each simulation must individually aggregate the resulting signal at the RAS equipment from each transmitter.

Following the Recommendation ITU-R M.2101 methodology, the BS and UE antenna normal vectors will, in general, be quasi-random (for BS this may be a known quantity in the planning process). As the direction to the RAS station (or to the local horizon in direction of the RAS station for trans-horizon paths) is usually not aligned with the AAS beam direction, the side-lobe gain of the antenna pattern in the direction of the RAS station must be determined accordingly, noting that this also depends on the current beam-forming direction as well as the 3D geometry and rotation angle of UE and BS devices.

The recommended method to determine the path propagation loss between the IMT equipment and the RAS station is provided in Recommendation ITU-R P.452 or Recommendation ITU-R P.2001. For the RAS station, the receiver gain specified for RAS protection criteria in Recommendation ITU-R RA.769 is for that of a 0 dBi side-lobe. If the antenna pattern for the RAS is needed, it could be obtained from Recommendation ITU-R SA.509, but in most cases of terrestrial sources of interference a flat level of 0 dBi should be used for reasons explained in Recommendation ITU-R RA.769, § 1.3 (see also *considering f)* and *g)* in that document). Topographic information, i.e. terrain height data, should be incorporated, as it has a significant effect on the diffraction loss in the Recommendation ITU-R P.452 or ITU-R P.2001 model, the calculation requires a specific terrain profile but may be suitable for Monte Carlo simulations by running the model repeatedly on real (but random) paths of a fixed length. Such paths should be chosen by using a terrain database for a region representative of the environment of interest (for example, by choosing a specific city to represent an urban area or choosing a specific mountain range to represent a mountainous area). Within this region, for each path a random starting point is generated, and the end point is calculated at a random azimuth, using the path length of interest. The propagation analysis is then performed on each path, and the Monte Carlo approach is used to derive the statistics of the loss for this path length. This can then be repeated for other path lengths. It is noted that Recommendation ITU-R P.452 or ITU-R P.2001 refers to Recommendation ITU-R P.676 for calculation of atmospheric losses. If available, atmospheric/weather data may be taken into account for more precise estimates of the atmospheric attenuation.

The deployment environments considered for IMT-2020 in the bands 24.25-86 GHz are outdoor Suburban hotspot, outdoor Suburban open space hotspot, outdoor Urban hotspot and Indoor. For the IMT stations operating on 42.5-43.5 GHz deployed in urban and suburban scenarios, Recommendation ITU-R P.2108, § 3.2 (Statistical clutter loss model for terrestrial paths) provides a statistical clutter loss model. In an aggregation calculation (Monte Carlo simulation) for each IMT device, a randomly chosen p_L value (uniformly distributed between 0 and 100%) should be used. As RAS antenna heights are usually very large, the Recommendation ITU-R P.2108 model should be used with a single-end point clutter model, i.e. for the IMT equipment only.

For the purpose of determining initial coordination distances for a given site, an IMT deployment model (enacted according to Recommendation ITU-R M.2101 methodology) providing desired coverage for IMT services should be used, noting IMT use of this band is focused on capacity rather than coverage.

To integrate the methodology of Recommendation ITU-R M.2101 into a derivation of coordination distances, a distance should be derived at which the Monte Carlo simulations do not exceed the protection criteria in Recommendation ITU-R RA.769. Additionally, no single transmitter in the network should produce a signal at the RAS site that exceeds these levels. The distance at which the aggregate signal no longer exceeds the threshold may be obtained through an iterative process; this represents an initial coordination distance.

To derive resulting signal strength for comparison with RAS protection criteria, the simulations performed under the Recommendation ITU-R M.2101 methodology must take several parameters into account, many of which are specific to individual sites. Primarily, these parameters impact the propagation of signals on the path from each simulated transmitter to the RAS receiver. Propagation characteristics used should be those typical for RAS observations at each site. For each signal path, the resulting signal may be found by:

$$P_R = P_T + G_R + \mathrm{G_T} + G_{BW} - PL - CL$$

where (all values in dB):

- P_R : power received by the RAS receiver (dBW)
- P_T : in-band transmitter power
- G_R : gain of the RAS telescope in the direction of the transmitter
- G_T : (side-lobe) gain of the IMT AAS in the direction of the RAS receiver (or the local horizon for trans-horizon paths) with ohmic loss accounted for
- G_{BW} : bandwidth correction factor for cases where the transmitter band is only partly overlapping the receiver band, or the receiver band is narrower than the transmitter band (e.g. in RAS spectral line observing mode)
- PL : path propagation loss, e.g. according to Recommendation ITU-R P.452 or ITU-R P.2001 (excluding clutter losses, but including atmospheric attenuation and diffraction loss due to the real terrain)
- CL : clutter losses (calculated per Recommendation ITU-R P.2108, § 3.2, or other appropriate models).

In calculating starting values for coordination distances at a given site, atmospheric characteristics using typical observing conditions may be employed to ensure coexistence. IMT deployments within the geographic range should proceed after coordination has taken place; this coordination process and evaluation may also account for local conditions, the specific power levels, siting and deployment, coverage patterns, and other factors for the specific IMT installation to prevent interference to an existing RAS site, as detailed in Annex 1.

4 Methodology: procedures and numerical framework for compatibility calculations

The methodology described in this section and the next is an example framework for addressing coexistence between IMT and RAS. This detailed methodology relies on the typical characteristics of both systems defined for the study cycle 2015-2019, and it is derived based on the generic methodology. It would also be possible to use simpler approaches, approximations or make other modifications where appropriate.

4.1 Worst case calculations

The calculations presented here are intended to bound the issue; by utilizing this methodology, the objective is 1) to provide administrations with the means to determine whether a compatibility issue is unlikely to present itself or 2) if a compatibility issue may occur, to provide administrations guidance on more site-specific characteristics and mitigation methods to ensure harmful interference does not occur. To produce this boundary analysis, several factors are assumed or not included, leading to “worst case” conditions.

The technical background for this work is found in Annex 1. Annex 2 contains an example application of the methodology provided in Annex 1.

The assumptions in these calculations include:

1) smooth earth (non-blocking) without terrain;

2) negligible atmospheric losses;

3) in-band (co-frequency) operation.

A sufficiently generic ‘boundary case’ deployment scenario could be chosen, conducted, and applied to all situations; however, to be more useful, some site-specific aspects may be incorporated, e.g. actual terrain. A more detailed analysis, utilizing local conditions, is expected to show compatible operation of IMT systems located within the boundary case as possible. Further modelling and use of a scenario with the expected size of the IMT deployment and proximity to the RAS site would also give a more accurate representation of compatibility. This approach thus does not derive a ‘minimum distance’ for compatibility between IMT and RAS systems; rather, it is used to determine whether a given proposed deployment may require additional measures to ensure compatibility. Examples of case studies (also with actual terrain) are contained in Annexes 3 and 4.

4.1.1 RAS station parameters

Threshold levels for interference detrimental to RAS are provided in Recommendation ITU-R RA.769. The total power into the RAS band, averaged over an integration time of 2 000 s, must not exceed a value of −191 dB(W/1 GHz), corresponding to the “continuum” protection criteria value. Consistent with Recommendation ITU-R RA.769, an isotropic antenna with a gain of 0 dBi is assumed when applying this criterion. If the antenna pattern for the RAS is needed, it can be obtained via Recommendation ITU-R SA.509.

4.1.2 IMT parameters

Representative IMT parameters may be found in ITU documentation (see Annex 1 to the Task Group (TG) 5/1 Chair’s Report). The typical deployment densities are defined as a function of the environment of the IMT BS and UE, urban or suburban hotspots. Antenna patterns to be used are found in Recommendation ITU-R M.2101.

4.1.3 Propagation and clutter models

For a generic boundary study, a flat (smooth-earth) propagation model found in Recommendation ITU-R P.452 or ITU-R P.2001 should be used, which refers to Recommendation ITU-R P.676 for some calculations related to atmospheric attenuation.

For the prediction of clutter loss, Recommendation ITU-R P.2108 should be employed if the IMT is deployed in suburban or urban areas. This model depends only on frequency, distance, and the location percentage, p_L. The variable p_L corresponds to the percentage of urban or suburban cases in which the clutter loss will be below the value calculated.

For the purposes of propagation in a generic scenario, typical atmospheric conditions (temperature: 20 °C, pressure: 1 013 mbar) should be assumed. At the frequencies in question, these conditions result in minimal atmospheric losses.

4.2 Aggregated power scenario

The aggregated power scenario considers the impact of the accumulated emitted power of all IMT devices around an RAS station. Here a Monte Carlo simulation is used to infer the total aggregate power of an ensemble of BS and UE devices, which are located randomly in a geographic area of sufficient size, adhering to the given distribution functions. This aggregated case is statistical in nature, therefore, small variations in the parameters and assumptions could lead to a significant change to the final result.

4.2.1 IMT deployment

The size of the IMT deployment and the proximity to the RAS station in question represent the primary degrees of freedom in the generic boundary study.

In Recommendation ITU-R M.2101 several possible deployment topologies are discussed, such as hexagonal or Manhattan-style grid layouts. Typical deployment number densities and other technical parameters were provided to ITU-R TG 5/1 (study cycle 2015-2019) and these references can be found in the Chair's Report of TG 5/1 (Document R15-TG5.1-C-0478). This group decided to use a uniform distribution of BSs. BSs are randomly sampled until the total number of devices leads to the specified BS number density over a wide area. From the perspective of a BS, the UE devices are distributed in a forward cone. One choice would be to distribute them following a radial and angular distribution function as defined in Annex 1 to the TG 5/1 Chair's Report. Another possibility would be to assume a distribution over a hexagonal cell grid as shown in Recommendation ITU-R M.2101. In the following, the former approach is used.

Then the distance between BS and UE is given by either a Rayleigh distribution or a log-normal distribution (for suburban open space). The angular distribution is given by a normal distribution, but with angles restricted within ±60°. The combination of both distributions defines the desired forward cone.

The Monte Carlo methodology used to calculate the aggregate power is straightforward: To each BS a random azimuthal orientation (bearing) is assigned during each Monte Carlo step, and it is assumed that only one sector is active per BS during a given step. In addition, each UE device can be rotated almost randomly, with the only restriction being that the UE-BS direction be located within ±60° from the antenna normal vector.

4.2.2 Effective antenna gains and propagation losses

To infer the effective antenna gains of the BS toward the RAS station it is necessary to calculate both the directions to the associated UE devices (yielding the Az_i and El_i steering direction of the beam), as well as to the RAS receiver, in the antenna reference frame. Likewise, for UE gains the direction to the BS and RAS receiver must be inferred in the UE antenna frame. This must be determined even for the spurious-domain cases (when studied), where single-element antenna patterns must be used, because the UE power control algorithm is based on coupling losses between UEs and BSs for which the effective gain of the array-antenna beams must be considered. As the BS and UE antenna frames are rotated and tilted, the calculations are best performed using 3D vector algebra and appropriate rotation matrices. It is noted that a typical BS has limited electrical steering ranges and the vertical limit has not been defined. For the direction to the RAS station, it is furthermore necessary to account for the path propagation horizon angle derived from the propagation loss calculation.

The gains described here must be re-calculated during each Monte Carlo step.

4.2.3 UE power control

IMT-2020 UE will be subject to power control. A more detailed description may be found in Annex 2.

4.2.4 Aggregated power at the RAS receiver

Each Monte Carlo iteration (i.e. one realization of a BS+UE configuration within the box) yields a total power level received at the RAS station, which is calculated by simply aggregating all individually emitted power levels and accounting for antenna gains and propagation losses. If boundary calculations show that Recommendation ITU-R RA.769 and Recommendation ITU-R RA.1513 thresholds are exceeded, additional analytical measures are needed to evaluate and facilitate compatibility. These measures may include a more detailed compatibility calculation (e.g. employing terrain blocking), as well as the employment of mitigation techniques (such as control of antenna orientation). These are discussed in the next section.

5 Further analysis and methods to enhance compatibility

5.1 Introduction

It is general consensus in spectrum management that both the interfering services, as well as the RAS, must work towards a situation that allows both stakeholders to peacefully coexist. On the RAS side, for example, Recommendation ITU-R RA.611 specifies “that radio astronomy observatories should continue to be placed in locations that have good natural protection from interference that may be detrimental to the RAS” and “that all practicable efforts should be made to minimize the side-lobe gains of radio astronomy antennas”. And, in fact, most modern RAS stations are operated in very remote places in order to minimize the impact of anthropogenic sources on astronomical observations.

More precise site-specific analysis, taking into account actual terrain and more in-depth consideration of climatological conditions for individual observatories, will provide additional data that may be used to facilitate sharing between IMT and RAS systems. This may be carried out in the iterative Monte Carlo simulations, and an example is set out in Annex 2 which follows the methods presented in Annex 1, or used after a coordination distance is identified to enhance compatibility.

5.2 Factors of interest to this analysis

5.2.1 Appropriate propagation conditions

Generally, atmospheric propagation in the subject frequency range is not a significant factor in reducing received aggregate signal power. However, using observed atmospheric characteristics for given RAS sites under realistic observing conditions, considering that such sites are typically located in remote locales selected for atmospheric conditions, may be warranted to assist with the coordination process.

Recommendation ITU-R P.452 or ITU-R P.2001 provides detailed calculation methodology for atmospheric loss employing empirical site-specific data.

It is well known that the topography around a RAS site has significant impact on the general interference situation. Diffraction at terrain is one of the most effective mitigation measures, especially at the high frequencies that are subject of this report. Unfortunately, existing RAS stations cannot be moved to different places and some sites, such as the WSRT in the Netherlands, are operated in a rather flat environment.

But, in general, the terrain can and should be incorporated in any coordination efforts, as it usually makes the required separation distances much smaller. The same is true for clutter, which can also provide additional path attenuation.

Recommendation ITU-R P.452 or ITU-R P.2001 provides information and procedures to account for multiple aspects of terrain loss, including knife-edge diffraction effects and spherical-Earth impacts. The most recent version of Recommendation ITU-R P.452, i.e. P.452-18, defines the use of both terrain heights and clutter categories along the radio-wave path and notes that if “the method is used to calculate diffraction loss using the terrain profile without clutter, the diffraction loss will be under-estimated in cluttered environments, as opposed to combined representation of terrain and clutter”. However, the use of Recommendation ITU-R P.452-17 with only a terrain profile along with the statistical clutter model in Recommendation ITU-R P.2108, § 3.2 will provide an alternative estimate of the desired basic transmission loss. Recommendation ITU-R P.2108 is of a statistical nature and can, for example, be used for IMT deployment in urban and suburban areas under the defined conditions with one or both of the radio transmitter and receiver terminals being embedded in local clutter (e.g. buildings).

Software solutions designed to incorporate terrain data may also be of use in facilitating compatibility between RAS observatories and IMT deployments.

5.2.2 IMT site planning

The general methodology for determining the need for mitigation methods described in the main body of this report is predicated on standardized deployment models. More site-specific deployments models, accounting for specific coverage needs for a given area, may provide both more realistic compatibility data and a means to vary parameters to resolve potential interference issues.

As explained above, the terrain and clutter around the RAS station play an important role. However, the path propagation equally depends on the situation at the transmitter, as the local terrain also provides diffraction (actually, any terrain features on the full propagation path are relevant.) Unless the BSs are installed at highly elevated antenna masts, clutter loss from objects around the transmitter applies; these could include houses, trees, etc. Placing IMT equipment such that local clutter is effective in the direction of the RAS station can make a significant difference. A transmitter attached to a wall on the opposite side of a house as seen from the RAS station will contribute much less to the received power than a transmitter on the facing side.

Site-specific characteristics, such as placing BSs so that main beam illumination covers a service area while pointing away from a RAS site, transmission power levels, lower deployment densities, and taking advantage of geographic characteristics (see § 5.2) may serve as factors which individually or in combination improve compatibility.

In some cases, ensuring compatibility may require minimum separation distances between the IMT deployment and RAS systems, regardless of other measures employed.

Terrain and clutter at any point in the propagation path from transmitter to receiver are relevant, and impact received signal through diffraction. Thus, clutter loss near transmitter, receiver, and at any point in between is relevant. IMT site planning such that clutter loss is increased toward nearby RAS sites may improve compatibility.

Once the baseline analysis of compatibility is conducted and a determination made that potential coordination issues may arise, a more computationally intensive further analysis accounting for more detailed modelling of a given site, including terrain, foliage, and other geographic factors, may be conducted. It may be desirable to conduct such an analysis in conjunction with the other factors detailed in this section.

5.2.3 AAS, beamforming, and antenna orientation

Modern 5G systems often utilize AAS, i.e. arrays of a large number of antenna elements. AAS allow to electronically form beams within its steerable limits directed towards the intended UE. This would, in principle, also allow to program the BSs in a way such that the location of an RAS station is avoided by the BS beam and its side-lobes. In addition, the array antenna could be mounted in a way such that it has large angular separation between its antenna normal and the location of the RAS station.

6 Summary

This Report provides: 1) an example of potential methodology to establish coordination zones around the RAS site operating in the 42.5-43.5 GHz frequency range to enhance compatibility with IMT systems operating in the mobile service allocation in the 37-43.5 GHz frequency range (that may be applied in co-frequency or adjacent-band cases); and 2) guidance that may enhance compatibility within coordination zones.

Annex 1

Technical background

This Annex contains procedures and formulae that can be used to determine the (aggregate) received power from an IMT BS and/or UE, or from a full network. It makes certain assumptions on the IMT characteristics (including its deployment) and modifications to the method described in the following should be considered when these assumptions do not apply. It is assumed that the BS locations are known, while the position of UE devices is quasi-random. For typical deployment densities in an IMT network and for information on how BS locations can be derived (if not yet known), see § A1.2.

Alternatively, similar procedures and calculation (simplified) can also be used by considering certain assumptions on the characteristics of the involved stations. A simplified approach could also offer equally valid results in certain cases, but this should be carefully tested against more sophisticated methods or real-world measurements if it is to gain higher confidence in the results. Simpler methods, however, would have the benefit of being less computationally demanding and potentially achieve similar results.

A1.1 Calculating effective transmitted IMT power towards RAS stations

A1.1.1 Introduction

Every BS can serve up to a given number of UE devices per frequency channel, which will use TDD, i.e. the up- and downlink communication occurs in time slots, which cannot be shared by different user devices. This also means that for a network simulation one needs to average the transmitted power from all devices over a sufficiently large period. To increase the link budget, the BS will dynamically steer its AAS beam towards each of the UE devices within the associated time slot. This also must be considered in a simulation by averaging over the effective antenna gains in time. Likewise, the UE may use AAS beamforming to improve the link budget. As the UE antenna frames can be arbitrarily rotated, the UE beams are also highly dynamic. It is usually assumed, however, that the angular distance between the UE antenna boresight and the actual direction to the host BS is, at most, 60° (otherwise, the UE antenna gain would be too low and the UE device would try to establish a connection to a different BS).

In the following, (u, v, h) will represent a Cartesian coordinate frame around the RAS station, with u measured to the East, v measured to the North, and h being the height above mean sea level (amsl). Thus, $(u, v, h)_{\mathrm{BS}}$ and $(u, v, h)_{\mathrm{UE}}$ are the positions of each individual IMT antenna. It is noted that Earth's curvature must be considered for radio wave propagation. This will be accounted for in a subsequent step. The (u, v, h) frame can be thought of as a local flat projection of the simulation area, akin to the Universal Transverse Mercator (UTM) or the European Terrestrial Reference System 89

(ETRS89) coordinate systems used in cartography. Each BS antenna sector will have a certain bearing (azimuthal direction), α_{BS}.

A1.1.2 Sampling UE positions in a BS sector

The UEs, which are linked to a certain BS, are not uniformly distributed. It is assumed that each BS serves a given sector covering 120° in azimuth. In this sector, the azimuthal distribution of the UEs is modelled with a normal distribution:

$$\rho(\varphi_{\mathrm{UE}}) = \frac{1}{\sigma\sqrt{2\pi}} \exp\left(-\frac{(\varphi_{\mathrm{UE}})^2}{2\sigma^2}\right) \quad \text{(A1-1)}$$

with $\sigma = 30°$ and φ_{UE} the azimuthal separation from the BS antenna frame boresight. However, positions shall be restricted to the interval $\varphi_{\mathrm{UE}} = [-60°, +60°]$, which means that when sampling from the distribution, values outside this interval must be discarded. This accounts for about 5% of the drawn samples.

For the radial distribution of the UEs, i.e. the distance, d_{UE}, on the ground between UE and BS, log-normal or Rayleigh distributions are usually employed. The former is recommended for open-space hotspots, while the latter shall be used for other types, i.e. for urban and suburban (outdoor) hotspots. The log-normal distribution is defined as:

$$\rho(d_{\mathrm{UE}}) = \frac{1}{d_{\mathrm{UE}}\sigma\sqrt{2\pi}} \exp\left(-\frac{(\ln d_{\mathrm{UE}} - \mu)^2}{2\sigma^2}\right) \quad \text{(A1-2)}$$

with $\mu = 3.9$ m and $\sigma = 0.42$ m. The Rayleigh distribution is given by:

$$\rho(d_{\mathrm{UE}}) = \frac{d_{\mathrm{UE}}}{\sigma^2} \exp\left(-\frac{d_{\mathrm{UE}}^2}{2\sigma^2}\right) \quad \text{(A1-3)}$$

with $\sigma = 32$ m.

A general method for sampling random numbers adhering to a distribution function is to sample uniformly distributed numbers, p, from the interval $p = [0, 1]$, and feed them into the inverse cumulative distribution function (CDF), which is also called the quantile function (QF). This technique is also known as "Inverse Sampling," and is a versatile tool for all sorts of random number generators. For continuous probability distributions it is not always possible to derive the QF in analytic form, but for discrete distributions (or approximations of continuous distributions) the strategy explained in § A1.4 can be employed.

The QF for the normal distribution is:

$$\varphi_{\mathrm{UE}}(p; \mu, \sigma) = \mu + \sigma\sqrt{2}\mathrm{erf}^{-1}(2p - 1) \quad \text{(A1-4)}$$

with the inverse error function, $\mathrm{erf}^{-1}(x)$. The QF for the log-normal distribution is:

$$d_{\mathrm{UE}}(p; \mu, \sigma) = \exp\left(\mu + \sqrt{2\sigma^2}\mathrm{erf}^{-1}(2p - 1)\right) \quad \text{(A1-5)}$$

likewise, the QF for the Rayleigh distribution is given by:

$$d_{\mathrm{UE}}(p; \sigma) = \sigma\sqrt{-2\ln(1 - p)} \quad \text{(A1-6)}$$

However, numerical libraries for most programming languages or math algebra software provide functionality to sample random values from these distributions, and it is usually recommended to use this for performance reasons.

After sampling the UE positions relative to the BS sector, the position in the global frame is given by:

$$u_{\mathrm{UE}} = u_{\mathrm{BS}} + d_{\mathrm{UE}}\cos\left(\alpha_{\mathrm{BS}} + \varphi_{\mathrm{UE}}\right)$$
$$v_{\mathrm{UE}} = v_{\mathrm{BS}} + d_{\mathrm{UE}}\sin\left(\alpha_{\mathrm{BS}} + \varphi_{\mathrm{UE}}\right)$$
$$h_{\mathrm{UE}} = h_{\mathrm{ground}}(u_{\mathrm{UE}}, v_{\mathrm{UE}}) + 1.5\ \mathrm{m} \qquad \text{(A1-7)}$$

where $h_{\mathrm{ground}}(u_{\mathrm{UE}}, v_{\mathrm{UE}})$ is the height of the terrain (amsl).

A1.2 Beamforming, geometrical calculations, and effective antenna gain

It was already discussed that both BS and UE AAS will be used to actively steer the beam towards the (currently active) counterpart. As the antenna frames are, in general, rotated with respect to the global coordinate frame, it is necessary to compute the beam positions in the antenna frame for each time step and device in order to derive the effective antenna gain in the beam direction and – equally important – the side-lobe gain towards the RAS station receiver. It is noted that the AAS gain pattern is highly dependent on the beam pointing.

Before the equations for this geometrical problem are presented, a few tools are introduced. The calculations can be performed very conveniently and efficiently using 3D linear algebra; in particular, employing rotation matrices. On the other hand, antenna gain formulae are often expressed in terms of spherical angles (i.e. azimuth and elevation). Hence, conversion between the Cartesian description and the spherical coordinate systems is necessary. Furthermore, as the antenna gain calculations are most easily done in the antenna pattern frames, a change of the basis frames is required, which is also discussed below.

A1.2.1 Spherical coordinates

A cartesian vector (x, y, z) can be converted to spherical coordinates (r, ϑ, φ) via:

$$r = \sqrt{x^2 + y^2 + z^2}$$
$$\vartheta = \frac{\pi}{2} - \arccos\left(\frac{z}{r}\right)$$
$$\varphi = \arctan\left(\frac{y}{x}\right) \qquad \text{(A1-8)}$$

where:

r : distance of a point to the coordinate centre

ϑ : elevation (not zenith distance) above the x-y plane

φ : angle between the projection of the vector (x, y, z) in the x-y plane and the x axis.

It is noted that in most computer software, the $\mathrm{arctan2}\ (y, x)$ function should be used to get the correct quadrant of the result. Below, the spherical coordinates (ϑ, φ), elevation and azimuth, will, for example, be required for determination of antenna gain values, as many ITU-R models work with spherical angles (and not with cartesian vectors). In this framework, the antenna normal points towards the (positive) x-axis, while y is the horizontal and z the vertical axis.

The inverse conversion formulae are:

$$x = r\cos\vartheta\cos\varphi$$
$$y = r\cos\vartheta\sin\varphi$$
$$z = r\sin\vartheta \qquad \text{(A1-9)}$$

For some applications, it can also be useful to calculate the true angular distance, σ, between two positions on a sphere:

$$\sigma(\varphi_1, \vartheta_1, \varphi_2, \vartheta_2) = \arccos\left(\sin\ \vartheta_1 \sin\ \vartheta_2 + \cos\ \vartheta_1 \cos\ \vartheta_2 \cos\left(\varphi_2 - \varphi_1\right)\right) \qquad \text{(A1-10)}$$

or the great circle bearing, α, under which Position 2 would appear as seen from Position 1:

$$\alpha(\varphi_1, \vartheta_1, \varphi_2, \vartheta_2) = \arctan\left(\frac{\cos\vartheta_2\ \sin(\varphi_2 - \varphi_1)}{\cos\vartheta_1 \sin\vartheta_2 - \sin\vartheta_1\cos\vartheta_2\cos(\varphi_2 - \varphi_1)}\right) \qquad \text{(A1-11)}$$

A1.2.2 Rotation matrices

All rotations in 3D cartesian space can be expressed as a 3 × 3 orthonormal matrix. It is $R^T R = 1$, which means $R^T = R^{-1}$. These can be conveniently constructed from successive applications of up to three elementary rotations:

$$R_x(\alpha) = \begin{pmatrix} 1 & 0 & 0 \\ 0 & \cos\alpha & -\sin\alpha \\ 0 & \sin\alpha & \cos\alpha \end{pmatrix}$$
$$R_y(\alpha) = \begin{pmatrix} \cos\alpha & 0 & \sin\alpha \\ 0 & 1 & 0 \\ -\sin\alpha & 0 & \cos\alpha \end{pmatrix}$$
$$R_z(\alpha) = \begin{pmatrix} \cos\ \alpha & -\sin\ \alpha & 0 \\ \sin\ \alpha & \cos\ \alpha & 0 \\ 0 & 0 & 1 \end{pmatrix} \qquad \text{(A1-12)}$$

which rotate any vector around the x, y, or z axis with a rotation angle α (in a mathematically positive sense). There are many different possibilities as to how this can be done which are beyond the scope of this Report. To name just two possibilities, one could use each of the three elementary rotations, e.g. $R = R_z(\gamma)R_y(\beta)R_x(\alpha)$, or just two of them, e.g. $R = R_z(\gamma)R_x(\beta)R_z(\alpha)$. Some of the many possible combinations are known as (classic) Euler angle representations.

An alternative method is to express a rotation via its (normalized) rotation axis, $\hat{r} = \vec{r}/|\vec{r}|$, and angle, α:

$$R = E + \sin(\alpha)W + 2\sin(\alpha/2)W^2 \qquad \text{(A1-13)}$$

where:

$$E = \begin{pmatrix} 1 & 0 & 0 \\ 0 & 1 & 0 \\ 0 & 0 & 1 \end{pmatrix},\ W = \begin{pmatrix} 0 & -\hat{r}_z & \hat{r}_y \\ \hat{r}_z & 0 & -\hat{r}_x \\ -\hat{r}_y & \hat{r}_x & 0 \end{pmatrix} \qquad \text{(A1-14)}$$

A1.2.3 Basis systems and basis change

The elements (values) of vectors and matrices are tied to the choice of a basis frame. When a basis frame is changed, e.g. when one converts between a global frame (such as the simulation box) and a local frame (rotated antenna frame), the new elements need to be calculated. As an example, consider a vector $\vec{x} = (x, y, z)$ in a given frame A. This vector can be rotated with a given rotation matrix R:

$$\vec{x}' = R\vec{x}(3.15) \quad \text{(A1-15)}$$

The resulting elements $\vec{x}' = (x', y', z')$, however, will still be in frame A. On the other hand, it is also possible to rotate the frame (with the same rotation matrix), resulting in frame B, and calculate the elements of the same vector $\vec{x}$ in the rotated frame:

$$\vec{x}^B = \begin{pmatrix} \vec{x} \cdot \hat{e}_{x_B} \\ \vec{x} \cdot \hat{e}_{y_B} \\ \vec{x} \cdot \hat{e}_{z_B} \end{pmatrix} = \begin{pmatrix} \vec{x} \cdot R\hat{e}_x \\ \vec{x} \cdot R\hat{e}_y \\ \vec{x} \cdot R\hat{e}_z \end{pmatrix} = R^T \vec{x}^A \quad \text{(A1-16)}$$

Likewise, because $R^T = R^{-1}$, it is also true that $\vec{x}^A = R\vec{x}^B$. It is also possible (and necessary) to change the elements of a matrix, M, if a basis change is performed:

$$M^B = R^T M^A R \quad \text{(A1-17)}$$

as can be seen when applying the matrix to a test vector (in frame B):

$$M^B \vec{x}^B = R^T M^A R \vec{x}^B = R^T M^A \vec{x}^A \quad \text{(A1-18)}$$

where in the first step, the vector is experiencing a basis change from B to A, then the matrix M (expressed in basis A) is applied, and finally the result is expressed in basis B by multiplication with R^T. In the following, this technique will make it possible to easily convert (and concatenate) antenna frame rotations in a very simple manner.

A1.2.4 Beam pointing in rotated frames

Every BS antenna is usually subject to an azimuthal rotation (bearing), α_{BS}, and potentially a mechanical down-tilt, $\varepsilon_{\text{tilt}}$. This can be represented as a concatenation of two elementary rotations:

$$R_{\text{BS}} = R_z(\alpha_{\text{BS}}) R_y(\varepsilon_{\text{tilt}}) \quad \text{(A1-19)}$$

It is noted that this rotation must not be applied to the global (u, v, h) coordinate of the BS, but to a device-local frame $(x, y, z)^{\text{nrl}}$. Before any rotation is applied, this non-rotated local (nrl) frame is aligned with the global (u, v, h) frame, but the origin is shifted to the antenna location. Likewise, the rotated local (*rl*) frame, $(x', y', z')^{\text{rl}}$ is defined, which stems from applying any rotation on the *nrl* frame about the origin of the *nrl* frame, i.e. the *nrl* and *rl* frames have an identical origin. The *rl* frame represents the actual antenna frames for quasi-randomly oriented antennas, while the *nr* frame is merely needed to convert device and antenna positions from *rl* to global (u, v, h) coordinates. For brevity, the notation (x, y, z) and (x', y', z') hereafter will be used for the *nrl* and *rl* frames, respectively.

For the UE, an arbitrary (random) 3D rotation R_{UE} acts on the device-local *nrl* frame. However, there exists the constraint that the maximum separation between the UE antenna boresight and the pointing vector to the host BS is less than 60 degrees (see above). There are three options to take this into account, with the first being the simplest, but the last being computationally more efficient and elegant.

Option 1: Create random rotation and discard samples

Sample three rotation angles from uniform distributions such that $\alpha_i \in [-180°, +180°]$, and compute:

$$R_{\mathrm{UE}} = R_z(\alpha_3) R_x(\alpha_2) R_z(\alpha_1) \tag{A1-20}$$

It is noted that other combinations of elementary rotations would also work and that the sphere is covered twice, i.e. for one angle α_2 it would suffice to use only angles from $[-90°, +90°]$. This rotation could now be applied to any vector of length 1, such as $\hat{e}_x$, to create a random position on the unit sphere, which shall represent the normal vector of the UE antenna frame. Using equation (A1-8) the corresponding azimuth and elevation angles $\left(\varphi^{\mathrm{nrl}}_{\mathrm{ant,UE}}, \vartheta^{\mathrm{nrl}}_{\mathrm{ant,UE}}\right)$ can be calculated.

Now, determine the vector between the UE and host BS:

$$\vec{n}_{\mathrm{UE}} = \begin{pmatrix} x \\ y \\ z \end{pmatrix}_{\mathrm{BS}\leftarrow\mathrm{UE}} = \begin{pmatrix} u \\ v \\ h \end{pmatrix}_{\mathrm{BS}} - \begin{pmatrix} u \\ v \\ h \end{pmatrix}_{\mathrm{UE}} \tag{A1-21}$$

where the meaning of the subscript "BS ← UE" is: "the direction to the BS, as seen from the UE." (The elements of the vector $\vec{n}_{\mathrm{UE}}$ are thus again defined in the device-local *nrl* frame). After normalization:

$$\hat{n}_{\mathrm{UE}} = \vec{n}_{\mathrm{UE}} / |\vec{n}_{\mathrm{UE}}| \tag{A1-22}$$

this can again be converted to azimuth and elevation angles $(\varphi_{\mathrm{BS}\leftarrow\mathrm{UE}}, \vartheta_{\mathrm{BS}\leftarrow\mathrm{UE}})$. Now the cases where the angular separation between the UE antenna normal and the direction to the BS (as seen from the UE) are larger than 60 degrees can be discarded, i.e. keep only samples with:

$$\sigma\left(\varphi_{\mathrm{ant,UE}}, \vartheta_{\mathrm{ant,UE}}, \varphi_{\mathrm{BS}\leftarrow\mathrm{UE}}, \vartheta_{\mathrm{BS}\leftarrow\mathrm{UE}}\right) \leq 60° \tag{A1-23}$$

This method is obviously somewhat inefficient, as more random samples need to be generated than are necessary. Furthermore, more complicated constraints may be more difficult to implement. It would also be possible to use a different procedure to create a unit vector on the sphere.

Option 2: Construct rotation matrix in world coordinates

Again, a rotation matrix will be constructed from three (non-elementary) rotations:

$$R = R_3(\alpha_3) R_2(\alpha_2) R_1(\alpha_1) \tag{A1-24}$$

Start from the hypothetical situation where the UE antenna normal was pointing to the host BS already, i.e. take $\hat{n}_{\mathrm{UE}}$ as defined in the method above. The first rotation matrix, $R_1(\alpha_1)$, shall perform a rotation about the UE-BS axis $(\vec{a}_1 := \hat{n}_{\mathrm{UE}})$ with angle $\alpha_1 \in [-180°, +180°]$. It can be computed using the axis-angle approach (see equation (A1-13). This rotation will leave the antenna normal vector untouched. Next, a rotation with a maximum angle of 60 degrees around any axis perpendicular to the UE-BS axis is applied. Without loss of generality, the axis lying in the (x, y) plane is used, as determined by:

$$\vec{a}_2 = \vec{a}_1 \times \hat{e}_z = \left(a_{1,y}, -a_{1,x}, 0\right) = (v_{\mathrm{BS}} - v_{\mathrm{UE}}, u_{\mathrm{UE}} - u_{\mathrm{BS}}, 0) \tag{A1-25}$$

Again, before equation (A1-13) can be used, the (rotation) axis vector must be normalised, i.e. use $\hat{a}_2 = \vec{a}_2/|\vec{a}_2|$ and rotate with α_2 randomly sampled from $[0°, +60°]$. Finally, rotate again about $\vec{a}_1$ with α_3 randomly sampled from $[-180°, +180°]$. Unlike in the first step, this time the UE-BS vector is not invariant under the rotation because the second rotation has tilted the coordinate frame away from the UE-BS axis.

Option 3: Construct rotation matrix in local frame and apply basis change

The method described in the previous section can also be constructed from two concatenated rotations. First, one can define a rotation that converts from the *nrl* frame to an initial frame (*"init"*), in which the antenna normal vector points to the host BS. Afterwards, the random UE rotation can easily be constructed using elementary rotation matrices only:

$$\tilde{R}_{\mathrm{UE}} = R_x(\alpha_3) R_y(\alpha_2) R_x(\alpha_1) \qquad \text{(A1-26)}$$

with $\alpha_{1,3} \in [-180°, +180°]$ and $\alpha_2 \in [0°, +60°]$. The initial rotation is given by:

$$R_{\mathrm{UE,nrl}\to\mathrm{init}} = R_z(\varphi_{\mathrm{UE-BS}}) R_y(-\vartheta_{\mathrm{UE-BS}}) \qquad \text{(A1-27)}$$

where $(\varphi, \vartheta)_{\mathrm{UE-BS}}$ is the spherical coordinate of the vector $\vec{n}_{\mathrm{UE}}$ in the *nrl* frame. To obtain the final UE rotation matrix (expressed in the *nrl* frame), a simple basis change is required:

$$R_{\mathrm{UE}} = R_{\mathrm{UE,nrl}\to\mathrm{init}} \tilde{R}_{\mathrm{UE}} R^T_{\mathrm{UE,nrl}\to\mathrm{init}} \qquad \text{(A1-28)}$$

A1.2.5 Determination of effective antenna gains

Several specific antenna gain values are necessary for aggregation simulations. For the UE power control algorithm, the link budget between UE and its host BS needs to be computed. For this, not only the path propagation according to 3GPP TR 38.901 (section 7.4.1) is considered, but also the antenna gains of the UE antenna (in direction of the host BS) and the gain of the BS antenna in the direction of the UE. In both cases, it is assumed that the beams are formed towards the communication partner, while the antenna normal are, in general, not pointing towards the other device. With the frame rotation matrices derived in the previous sections, it can be found for the UE position expressed in the BS frame (*rl*):

$$\begin{pmatrix} x' \\ y' \\ z' \end{pmatrix}_{\mathrm{beam,UE}\leftarrow\mathrm{BS}} = R^T_{\mathrm{BS}}(-\vec{n}_{\mathrm{UE}}) \qquad \text{(A1-29)}$$

where the meaning of the subscript "UE ← BS" is: "the direction to the UE, as seen from the BS." Likewise, the BS position expressed in the UE frame (*rl*) is:

$$\begin{pmatrix} x' \\ y' \\ z' \end{pmatrix}_{\mathrm{beam,BS}\leftarrow\mathrm{UE}} = R^T_{\mathrm{UE}}\, \vec{n}_{\mathrm{UE}} = \tilde{R}^T_{\mathrm{UE}} \begin{pmatrix} 1 \\ 0 \\ 0 \end{pmatrix} \qquad \text{(A1-30)}$$

in which the last equality is a trivial consequence of the choice of frames in Option 3 above.

The effective antenna gains can be calculated by converting the resulting cartesian vectors, which are expressed now in the *rl* antenna frames, to spherical angles $(\varphi'_{\mathrm{beam}}, \vartheta'_{\mathrm{beam}})$ and feeding these into the AAS pattern of Recommendation ITU-R M.2101 Table 4 for both the actual angles[2], $(\varphi, \theta) = (\varphi'_{\mathrm{beam}}, 90° - \vartheta'_{\mathrm{beam}})$, and the beam position, $(\varphi_{i,\mathrm{escan}}, \theta_{i,\mathrm{tilt}}) = (\varphi'_{\mathrm{beam}}, -\vartheta'_{\mathrm{beam}})$.

The same must be done for the effective gain of the BS and UE antenna patterns in the direction of the RAS station. As both the terrain heights and the curvature of the Earth do play a role, in a first step, the bearing angles towards the RAS station as well as the local horizon elevation angles must be determined. These are usually calculated as a by-product in the path propagation (pp) calculations as proposed in Recommendation ITU-R P.452-17, for example. It is denoted the direction to the RAS station as $(\varphi, \theta)_{\mathrm{pp}}$ (in *nrl* frame)[3].

To calculate the gain, this position needs to be expressed in the antenna frames, i.e.:

$$\begin{pmatrix} x' \\ y' \\ z' \end{pmatrix}_{\mathrm{Rx} \leftarrow \mathrm{BS}} = R^T_{\mathrm{BS}} \vec{x}_{\mathrm{pp,BS}}$$

$$\begin{pmatrix} x' \\ y' \\ z' \end{pmatrix}_{\mathrm{Rx} \leftarrow \mathrm{UE}} = R^T_{\mathrm{UE}} \vec{x}_{\mathrm{pp,UE}} \qquad \text{(A1-31)}$$

where $\vec{x}_{\mathrm{pp,BS}}$ and $\vec{x}_{\mathrm{pp,UE}}$ are the cartesian vectors associated with $(1, \varphi_{\mathrm{pp}}, \theta_{\mathrm{pp}})$ at the BS and UE positions. As before, the gains can now be determined using Recommendation ITU-R M.2101.

---

2 It is noted that Recommendation ITU-R M.2101 uses azimuth, φ, and zenith angle (wrongly referred to as elevation), $\theta = 90° - \vartheta$, instead of elevation angle, ϑ. In contrast, the tilt angle, $\theta_{i,\mathrm{tilt}}$, is not used as a zenith angle, but as elevation with opposite sign.

3 In Recommendation ITU-R P.452-17, the azimuthal direction to the receiver is given by α_{tr} (their equation (67)), while the transmit elevation angle is denoted as θ_t (their equation (154)). However, α_{tr} is defined with respect to North, while the (u, v, h) system used in this Report is with respect to East, i.e. $\varphi_{\mathrm{pp}} = 90° - \alpha_{tr}$.

FIGURE A1-1

Coordinate frames of BS and UE antennas

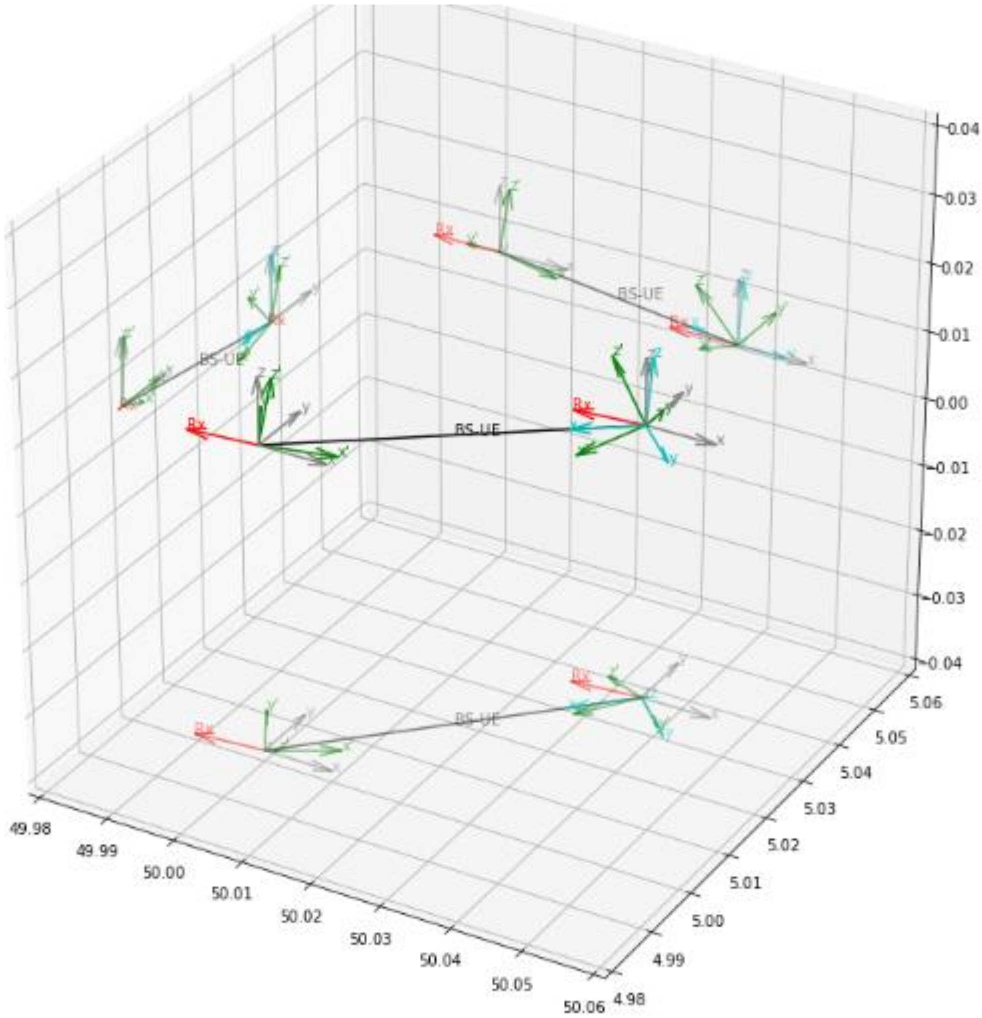

The various coordinate frames are visualized in Fig. A1-1. The axes show the global (u, v, h) coordinates, with the RAS station located at the origin of this frame. There is one BS at position (50 km, 5 km, 6 km) with a bearing angle of $\alpha_{\mathrm{BS}} = 30°$ and a down-tilt of $\varepsilon_{\mathrm{tilt}} = 10°$. A UE device is placed at a distance of $d_{\mathrm{UE}} = 50$ m with an azimuthal angle of $\varphi_{\mathrm{UE}} = 15°$ into the BS antenna footprint. Thus, the global position of the UE is $(u, v, h)_{\mathrm{UE}} = (50.0354\ \mathrm{km}, 5.0354\ \mathrm{km}, 1.5\ \mathrm{m})$. All terrain heights are assumed to be zero. For the UE rotation, the angles $(\alpha_1, \alpha_2, \alpha_3) = (10°, 20°, 30°)$ are used. In Fig. A1-1, the grey arrows show the *nrl* frames at the BS and UE positions, respectively. The green arrows indicate the antenna (*rl*) frames. For illustration, the *init* frame is also displayed, in which the UE antenna normal is pointing to the BS. Red arrows mark the path propagation vector towards the RAS receiving station.

In order to apply Recommendation ITU-R P.452-17, the BS and UE positions must be known in WGS84 longitudes and latitudes, (l, b). For the example in Fig. A1-1, it is assumed that the RAS station is at $(l, b)_{\mathrm{Rx}} = (7°, 50°)$. As previously mentioned, one can utilise a local flat projection such as UTM to convert between (u, v, h) and WGS84 coordinates. Then, $(l, b)_{\mathrm{BS}} = (7.6962°, 50.0549°)$ and $(l, b)_{\mathrm{UE}} = (7.6967°, 50.0552°)$. Recommendation ITU-R P.452 predicts:

$$\left(\varphi_{\mathrm{pp}}, \theta_{\mathrm{pp}}\right)_{\mathrm{Rx}\leftarrow\mathrm{BS}} = (-173.290°, -0.069°) \text{ and } \left(\varphi_{\mathrm{pp}}, \theta_{\mathrm{pp}}\right)_{\mathrm{Rx}\leftarrow\mathrm{UE}} = (-173.254°, -0.034°).$$

FIGURE A1-2

Phased-array antenna gain for BS and positions of the formed beam (black circle) and RAS station (red circle)

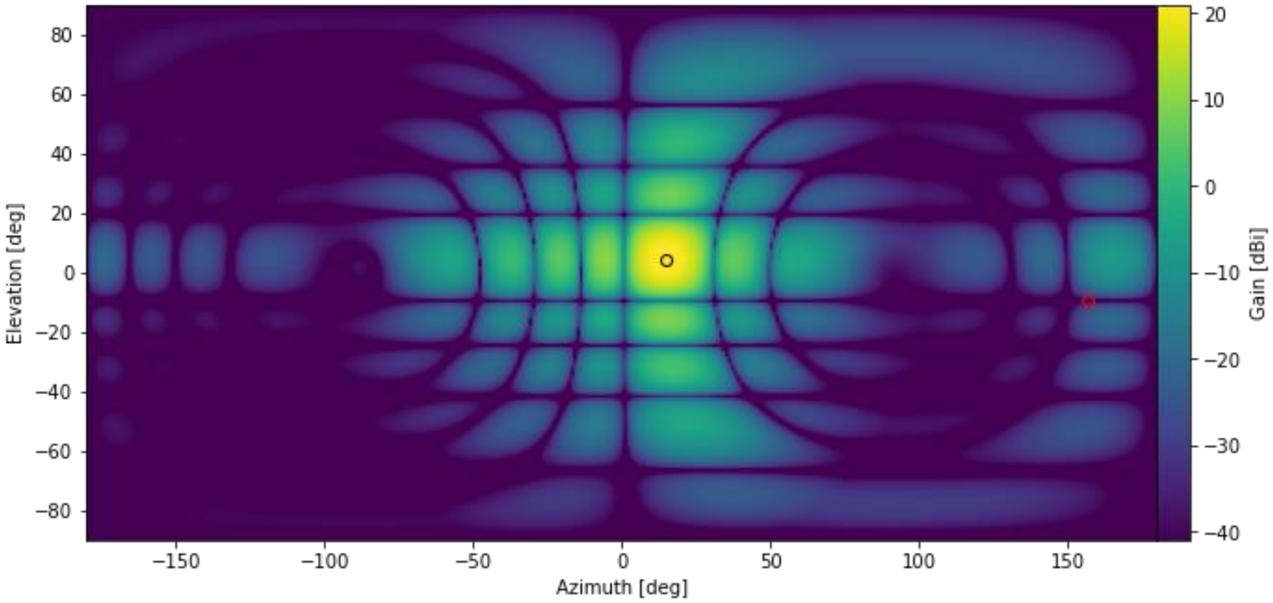

Based on this it is found for the UE device position in the BS antenna frame (*rl*), $(\varphi'_{\text{beam}}, \theta'_{\text{beam}})_{\text{UE}\leftarrow\text{BS}} = (14.986°, 4.518°)$, and for the RAS position (or rather the propagation path's position) $\left(\varphi'_{\text{pp}}, \theta'_{\text{pp}}\right)_{\text{Rx}\leftarrow\text{BS}} = (156.385°, -9.246°)$, respectively. The former is marked with a black circle in Fig. A1-2, while the latter is indicated with a red circle.

FIGURE A1-3

Phased-array antenna gain for UE and positions of the formed beam (black circle) and RAS station (red circle)

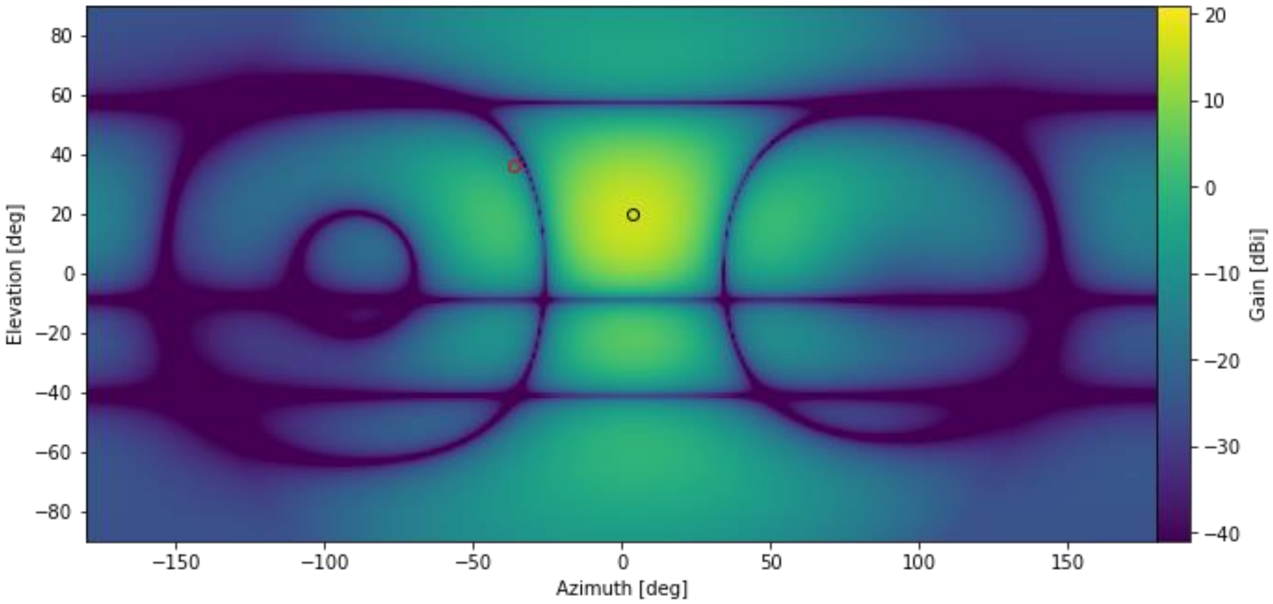

Likewise, the beam (to the BS) and RAS Rx positions in the UE frame (*rl*) are, $(\varphi'_{\text{beam}}, \theta'_{\text{beam}})_{\text{BS}\leftarrow\text{UE}} = (3.616°, 19.683°)$ and $\left(\varphi'_{\text{pp}}, \theta'_{\text{pp}}\right)_{\text{Rx}\leftarrow\text{UE}} = (-36.219°, 36.319°)$; see Fig. A1-3.

A1.3 Sampling BS locations according to land cover types

For generic aggregation studies, one of the first steps in the calculations is to simulate the deployment of BSs and UEs. In Recommendation ITU-R M.2101, several possible IMT network topologies are discussed, such as hexagonal or Manhattan-style grid layouts. However, typical deployment number densities and other technical parameters vary with the target IMT frequency band and technology generation. Such numbers are usually provided by the involved working parties.

For generic simulations, the provided IMT parameters usually include typical device densities for the relevant land-cover type zones, such as urban/suburban or rural areas. However, in most cases, no specifications are made with respect to the spatial distribution functions of devices. This usually has to do with the fact that for small-area simulations a single zone type can be assumed, and within these it makes sense to work with a relatively homogeneous deployment, as proposed in Recommendation ITU-R M.2101. For very large areas, the actual distribution usually has a less significant impact on the (statistical) results. For RAS, however, one can think of setups where the actual “clustering” of urban/suburban zones might play a role. Indeed, RAS stations are often in remote areas, but there could be some smaller towns nearby which would introduce a strong direction dependence with regards to minimum separation distances.

Technically, some of the IMT studies make a difference between built-up area (i.e. having housings), in which (sub)urban zones are embedded, while in other studies – especially at lower frequencies – IMT BSs could also be deployed anywhere (i.e. also in rural areas) not necessarily associated with housings. In the following, as this Report is about 5G at mm waves, the former scenario will be used. For mm-wave 5G it is furthermore expected that BSs will only be installed in (sub)urban areas. The fraction of the total area that contains housings is usually denoted as R_b. Within this, only a part of the area is thought to have urban or suburban land cover. This fraction is the so-called R_a parameter.

The following method is an example to create detailed zone maps. It is based on the observation that densely populated areas, such as cities and towns, cover a certain (connected) area. In addition, suburban areas often surround urban cores in a city. Such spatial correlations can be introduced numerically in different ways, but one of the easiest methods is to smooth-down a map consisting of uncorrelated noise samples.

FIGURE A1-4

Creating pseudo-land-cover class zones by creating a spatially correlated noise map and applying thresholds

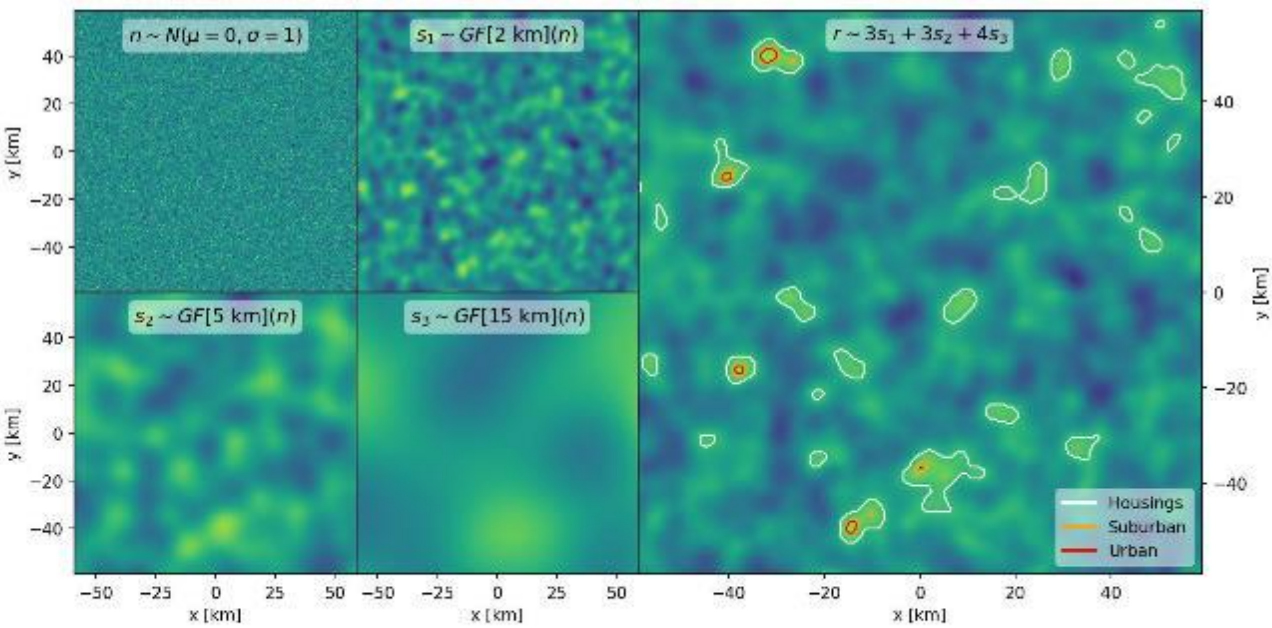

The method is visualized in Fig. A1-4. The individual steps are:

1) Create a map of spatially uncorrelated noise, e.g. by drawing random samples from a normal distribution (independently for each pixel); see top left panel of Fig. A1-4.

2) Apply a spatial filter, such as a Gaussian filter, $GF[\sigma_m]\big(n(x,y)\big)$, with various kernel sizes, σ_m. In the example in the Figure, the kernel sizes $\sigma_m = 2, 5,$ and 15 km have been used.

3) Sum the smoothed-down versions of the map. Applying weighting factors is an option and can be used to give certain distance scales more impact. The result of this is shown in the right panel of Fig. A1-4.

4) Apply thresholds based on the percentile levels associated with the required housing (R_b) and/or area ratios (R_a). In the example, $R_b = 5\%$, and $R_a^{\mathrm{urban}} = 7\%$ and $R_a^{\mathrm{suburban}} = 3\%$, respectively, i.e. the lowest threshold – which defines the housing area – is at 95% ($= 100\% - R_b$), while the threshold for suburban areas is at 99.5% ($= 100\% - R_b(R_a^{\mathrm{urban}} + R_a^{\mathrm{suburban}})$) and for urban it is at 99.65% ($= 100\% - R_b R_a^{\mathrm{urban}}$). Obviously, the area marked as "suburban" also includes the "urban" areas, such that the "highest" zone type should be used subsequently for each pixel in the simulation box.

The result can also be displayed in a different style, without contours, as in Fig. A1-5. The next task to be addressed is how to sample BS locations into the simulation box, such that the given number densities and land cover types are respected. For this, again, the "inverse sampling" procedure can be used, which is discussed in § A1.4. The method also works for n-dimensional data. The 2-D land cover map can be transformed into a number density map by assigning a (fixed) number density to each pixel according to the zone type. This density map can be understood as a discrete two-dimensional probability distribution, if it was normalized. Hence, the inverse sampling is realized by flattening the map (i.e. create a 1-D array consisting of the rows of the map), computing the cumulative sum, and dividing the result by the sum of all densities (or by the last element of the cumulative-sum array). To illustrate this, a toy map has been created with just one of each zone type (see Fig. A1-6). If the pixel grid is relatively coarse, it is furthermore a viable strategy to add some sub-cell random shifts to each location. This helps to keep the computational costs small while not losing much accuracy.

FIGURE A1-5

Result of the procedure depicted in Fig. A1-4 with the various zone types highlighted as coloured regions

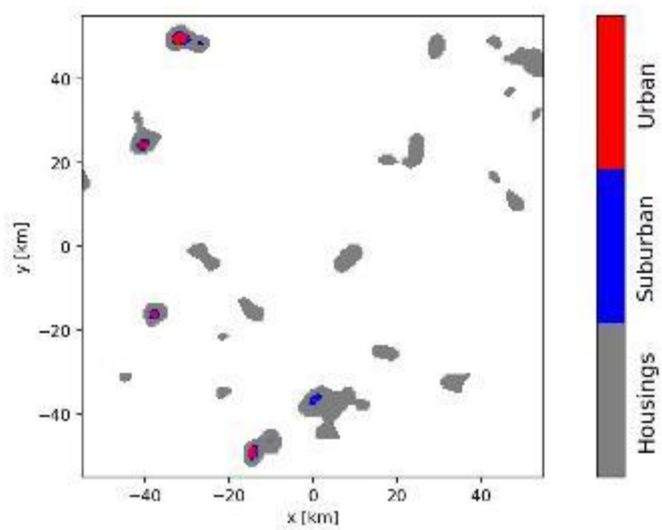

FIGURE A1-6

Sampling BSs into different zones. The BS number densities are 10 / km² for suburban and 30 / km² for urban zones

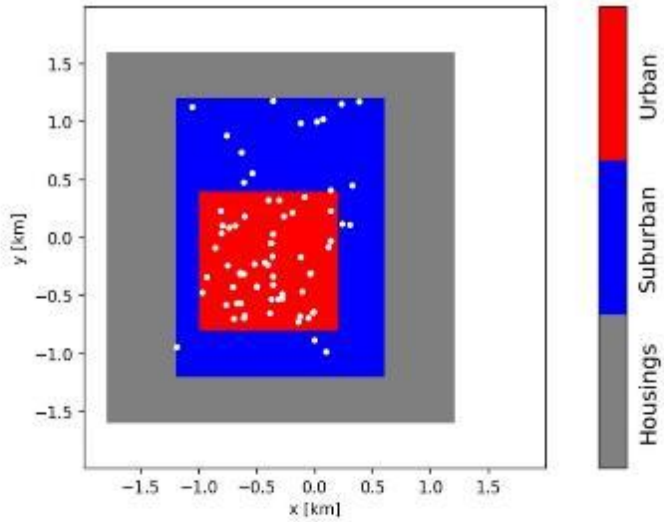

A1.4 Inverse sampling

If one needs to sample random numbers adhering to a given probability distribution, the "inverse sampling" technique can be used. Here the discrete version is explained, which works with any discrete probability distribution, $\rho(x)$, and can also be used to approximate continuous cases. The basic idea is sketched in Fig. A1-7. Mathematically, the inverse CDF, F^{-1}, is determined and random numbers from the uniform distribution are fed into it:

$$x_n \sim F^{-1}(y_n), \quad \text{with } y_n \sim U(0,1) \text{ and } F(x) = \int_0^x \rho(x')dx'. \tag{A1-32}$$

For discrete distributions or numerical approximations, the integral is replaced with the sum, in which case $F(x)$ becomes the cumulative sum of $\rho(x)$. Taking the inverse is then a search operation in the CDF curve, i.e. finding the piece of the curve having the required y_n-value, which gives the associated x_n.

The inverse sampling technique can be used to generate random numbers adhering to a given target probability distribution by using the inverse CDF (or an approximation of it) and feeding in uniformly distributed random samples.

FIGURE A1-7

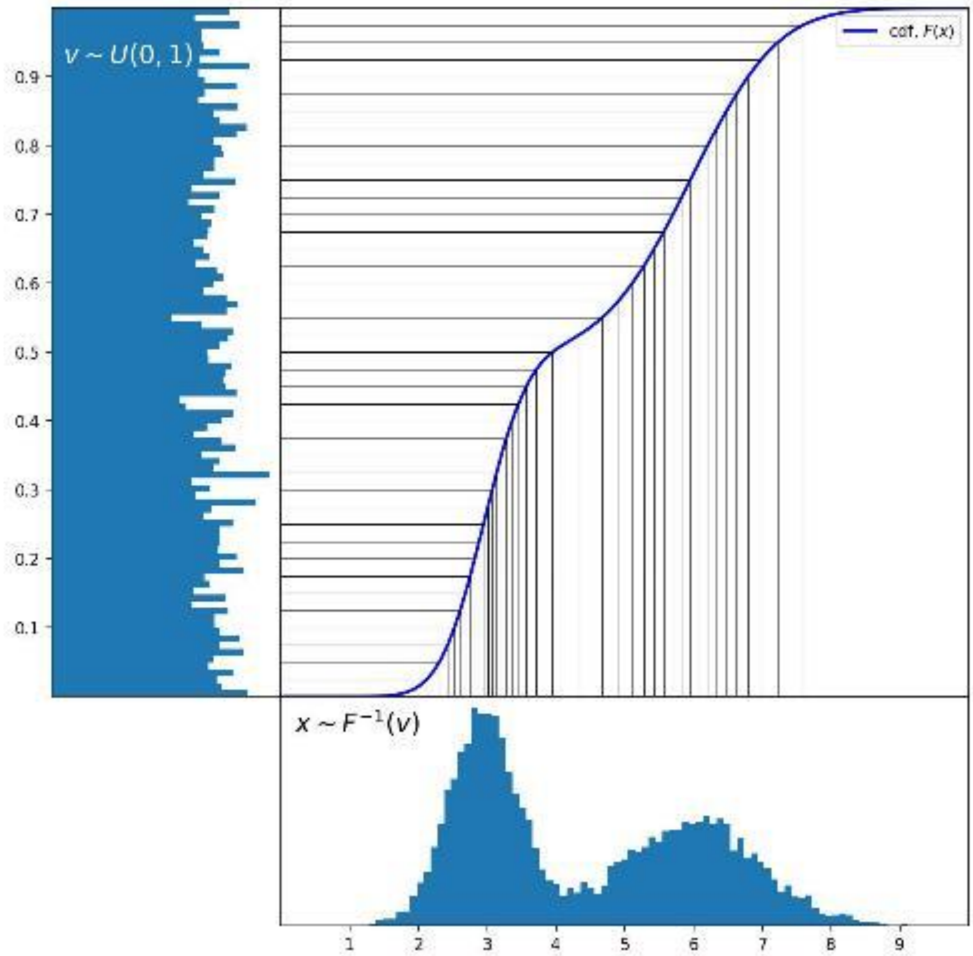

Annex 2

Generic example and case study calculations

Examples included herein are intended as guidance to administrations for implementation of the example methodology detailed in this Report. They are not intended as sharing and compatibility studies toward regulatory proceedings, and are theoretical studies with certain assumptions of the IMT characteristics, which may deviate from the properties of actual deployment. For real RAS station sites, terrain information should be included and the planned or actual IMT device deployment could be incorporated, too, without a significant change of the method.

A2.1 Generic (flat-terrain) single-entry and aggregation simulations

This Annex contains generic sharing and compatibility studies between the RAS in the frequency band 42.5-43.5 GHz with IMT in the frequency band 40.5-43.5 GHz based on a (flat-terrain) aggregation simulation.

A2.1.1 Study parameters

A2.1.1.1 RAS station parameters

The IMT frequency band 40.5-43.5 GHz is, in part, adjacent to and shared with the RAS frequency band 42.5-43.5 GHz (primary allocation). Threshold levels for interference detrimental to RAS are provided in Recommendation ITU-R RA.769. The total power into the RAS band, averaged over an integration time of 2 000 s, must not exceed a value of −191 dB(W/1 GHz). In this study, only the case of broadband (“continuum”) RAS observations is considered. For the RAS station an isotropic antenna with a gain of 0 dBi with a height of 50 m above the ground is assumed, as proposed by Recommendation ITU-R RA.769.

A2.1.1.2 IMT parameters

The IMT parameters were listed in the main part of this Report, but the values, which are actually used for the study below, are summarized in Table A2-1 for convenience. The typical deployment densities are defined as a function of the environment of the IMT BSs and UEs, urban or suburban hotspots. The BSs are usually not operating at 100% of their maximum capacity. In the calculations a network loading factor of 20% is assumed. The TDD activity factors are 80% for BSs and 20% for UE. Antenna patterns are taken from Recommendation ITU-R M.2101.

The total integrated gain correction factors listed in Table A2-1 are based on the guidelines provided in Annex 1 to the TG 5/1 Chair’s Report. For the composite antenna patterns, the factors were calculated for the beam formed in forward direction only.

TABLE A2-1

IMT technical parameters for BSs and UEs

Parameters	IMT BS	IMT UE
Frequency	41.5 GHz	41.5 GHz
Antenna	8 × 16 array elements, 65° 3-dB width, G_{elem}=5 dBi, 30 dB f/b ratio, λ/2 spacing	4 × 4 array elements, 90° 3-dB width, G_{elem}=5 dBi, 25 dB f/b ratio, λ/2 spacing
Total integrated gain correction	+4.83 dB (single element) +0.28 dB (composite beam)	+2.44 dB (single element) +0.33 dB (composite beam)
Tilt	−15° (suburban open space), −10° (urban/suburban)	0°
Ptx (1)	10 dBm per element	10 dBm per element
Antenna height	15 m (suburban open space), 6 m (urban/suburban)	1.5 m
Spectral mask	−56 dBc (spurious gain)	−49 dBc (spurious gain)
Ohmic losses	−3 dB	−3 dB
Other losses	n/a	4 dB (body loss)
Total radiated spectral power density in RAS frequency band (1), (2)	−30 dB(m/MHz) (spurious) 3 dB(m/MHz) (in-band)	−30 dB(m/MHz) (spurious) −4 dB(m/MHz) (in-band)
Total radiated power into RAS frequency band (2), (3)	0 dBm (spurious) 26 dBm (in-band, one carrier)	0 dBm (spurious) 19 dBm (in-band, one carrier)
Network loading factor	20%	n/a
TDD activity factor	80%	20%
Rb (housing ratio)	5%	5%

TABLE A2-1 (*end*)

Parameters	IMT BS	IMT UE
Ra (ratio of hotspot area to housing area)	7% (urban), 3% (suburban)	7% (urban), 3% (suburban)
Deployment density in hotspot area	30 km^{-2} (urban), 10 km^{-2} (suburban), 1 km^{-2} (suburban open space)	100 km^{-2} (urban), 30 km^{-2} (suburban)
Distribution of UE (relative to BS)		
Distance distribution	log-normal(0.42, 3.9) (suburban open space) Rayleigh(0, 32) (urban/suburban)	
Angular distribution	normal(0, 30) (clipped at ±60°)	

(1) The UE maximum transmit power will be lower in some simulation instances as it is subject to the power control algorithm.

(2) (Spectral) TRP values in the Table do not include UE body losses.

(3) Within the RAS bandwidth of 1 GHz up to five carriers/channels of 200 MHz could be active.

A2.1.1.2.1 Base stations

The BSs utilize 8 × 16 antenna elements, each with Ptx = 10 dBm. For the adjacent-band (spurious emission) case, the considered RAS frequency band is in the spurious domain ($\Delta f \geq 400$ MHz) with respect to the 40.5-42.5 GHz MS frequency band under consideration. The spurious emission (TRP) in the RAS frequency band is −30 dB(m/MHz), which is equivalent to 0 dBm over the full RAS bandwidth of 1 GHz. In-band, the array has a TRP of 26 dBm (3 dB(m/MHz)) for every IMT carrier active in the RAS band. However, within the RAS bandwidth of 1 GHz, up to five carriers/channels of 200 MHz could be active. The e.i.r.p. levels can be significantly higher, depending on the beam direction of the AAS.

For compatibility studies with the RAS in the spurious domain the single-element antenna pattern is to be used (see Fig. A2-1), whereas for the in-band sharing calculations the composite antenna pattern is to be used, which depends on the position of the formed beam. In Fig. A2-2, the example of $(Az, El)_{beam} = (0°, 0°)$ is shown. The antenna patterns are defined in Recommendation ITU-R M.2101. However, the given equations are not properly normalized (the average over the full sphere should be one, i.e. 0 dBi). The correction factors are denoted as “total integrated gain corrections” and are provided in Table A2-1.

FIGURE A2-1

Antenna gain of a single element of an IMT BS

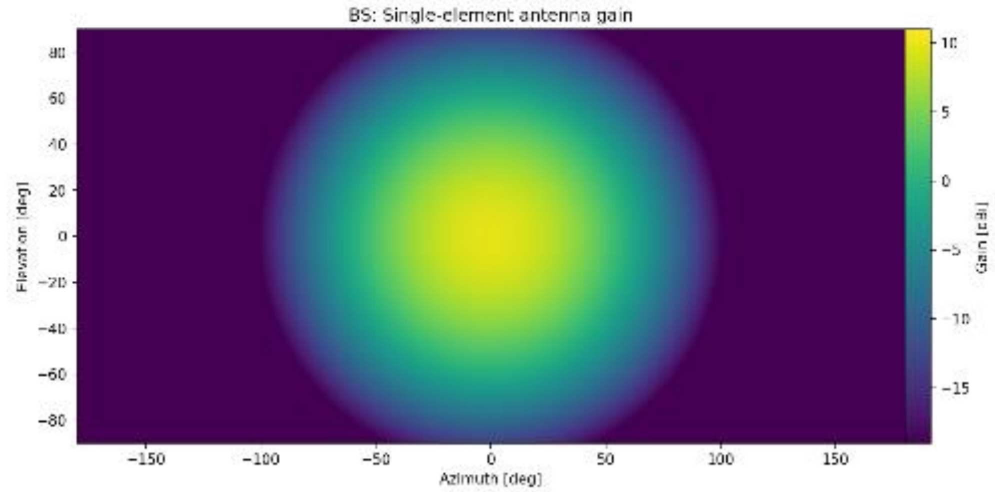

FIGURE A2-2

Composite antenna gain of an IMT BS

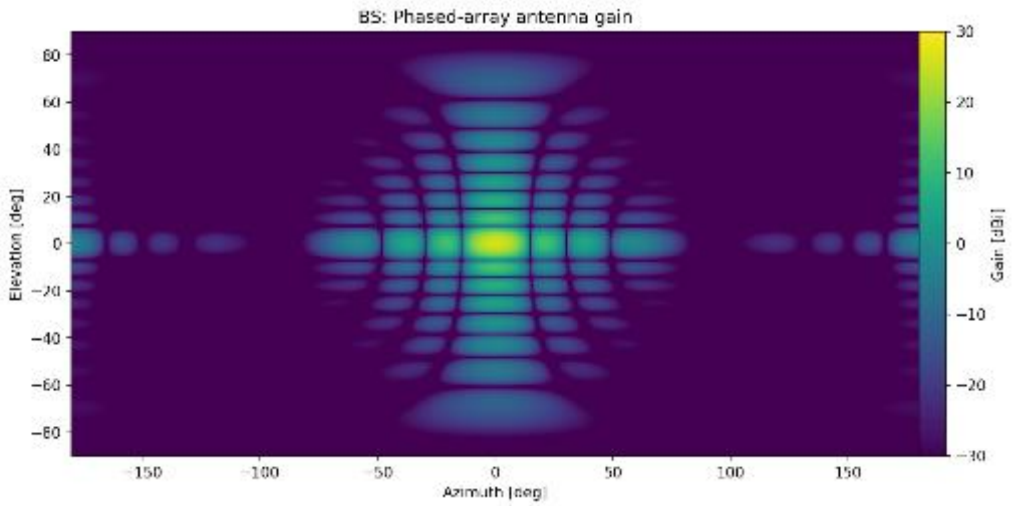

For BS, different antenna heights must be considered, depending on the environment (urban or suburban). To improve the gain after beamforming, the arrays are furthermore slightly tilted with respect to the horizon.

A2.1.1.2.2 User equipment

Compared to the BSs, the UEs have fewer elements (4 × 4) contained in an array, but with the same transmitting power of 10 dBm. Since the spectral side-lobe suppression is somewhat less effective, the UE spectral TRP in the spurious domain is also −30 dB(m/MHz). Additionally, 4 dB body absorption loss is considered. The in-band TRP is 19 dBm (−4 dB(m/MHz)) for a single carrier and 26 dBm if IMT carriers are active over the full RAS band.

The UE single-element antenna gain is visualised in Fig. A2-3, and an example composite antenna pattern with the beam formed in the forward direction is shown in Fig. A2-4. The UE will have antenna arrays on the front and the back, and it is assumed that all UE antenna frame normal vectors will be pointing, at most, 60 degrees away from the direct sight lines to their associated BSs.

FIGURE A2-3

Antenna gain of a single element of an IMT UE

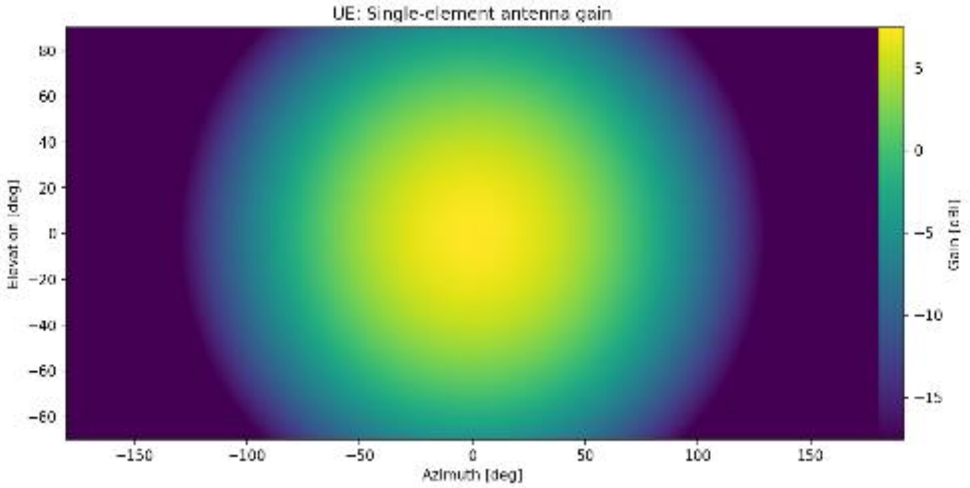

FIGURE A2-4

Composite antenna gain of an IMT UE

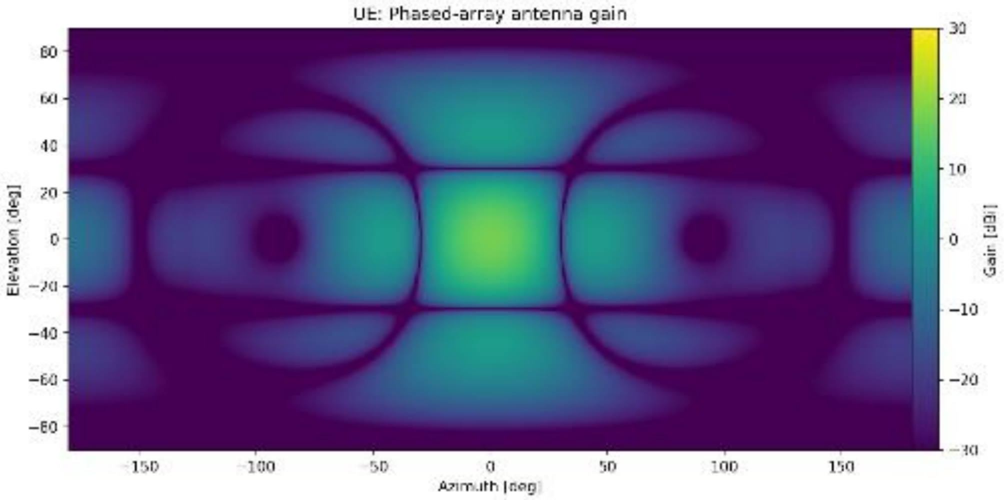

A2.1.1.3 Propagation and clutter models

For this compatibility study, a flat (smooth-earth) propagation model according to Recommendation ITU-R P.452-16 is used, accounting for the relative angle between the propagating path and the boresight of the IMT antenna elements (including BS tilt and UE rotations) that influences the effective antenna gain. Furthermore, for the in-band case, where the composite antenna pattern has to be used, the position of the formed beam changes the effective gain towards the RAS station. Further details on this are discussed in § A2.3.2. The 'time percentage' parameter p, which is defined in Recommendation ITU-R P.452-16, was set to 2%. This means that the actual path propagation loss will be less for 2% of the time. This was done following *recommends* 2 of Recommendation ITU-R RA.1513, which states that RAS must accept 2% data loss.

For the deployment of IMT equipment around RAS stations, case studies for individual RAS stations may be required, which can only be performed using detailed and specific information about deployment scenarios for IMT equipment.

For the prediction of clutter loss, Recommendation ITU-R P.2108, § 3.2 was used. This model depends only on frequency, distance, and the location percentage, p_L. The latter quantity is to be understood as the percentage of emitters (spread across an urban or suburban zone) producing the lowest clutter loss. For example, if p_L is 2%, (i.e. adopting a worst-case scenario) the value returned by the method indicates that for 2% of all cases the clutter loss will be lower than the value. It must be noted that the model in Recommendation ITU-R P.2108, § 3.2 is appropriate for urban and suburban land cover types only if the IMT devices are being embedded in local clutter, e.g. buildings. In the following, the results for zero clutter loss values will also be provided for comparison even though a zero clutter loss assumption is unrealistic in practice.

At 43 GHz and for distances larger than 5 km, clutter loss values for p_L = 2% are approximately 27 dB, whereas up to 20 dB clutter attenuation is assumed in this study based on Recommendation ITU-R P.452-16. The most recent version of Recommendation ITU-R P.452, i.e. P.452-18, introduces a new clutter loss method that has not been implemented in this study. In the case of aggregate emissions, an integration of received powers over a sufficiently large area will be performed. Therefore, random p_L values ranging from 0% to 100% are assigned to each BS and UE device. The expectation value of the clutter loss distribution for distances larger than 5 km is 35.0 dB at 43 GHz.

Typical atmospheric conditions (temperature: 20° C, pressure: 1 013 mbar) were assumed. For IMT equipment, the path attenuation is dependent on the associated zone (urban/suburban), as the BS antenna heights vary and have an impact on the attenuation. The resulting path attenuation values are displayed in Figs A2-5 and A2-6 for UE and BS, respectively, as dashed lines. Additionally, there are two curves for the total path attenuations including Recommendation ITU-R P.2108 clutter: one for the expected value of the clutter loss, and another for the p_L=2% case. For UE, an additional 4 dB of body absorption loss must be taken into account, which is not included in the figures.

FIGURE A2-5

Path attenuation of UE as a function of distance to the RAS station obtained using Recommendations ITU-R P.452-16 and ITU-R P.2108

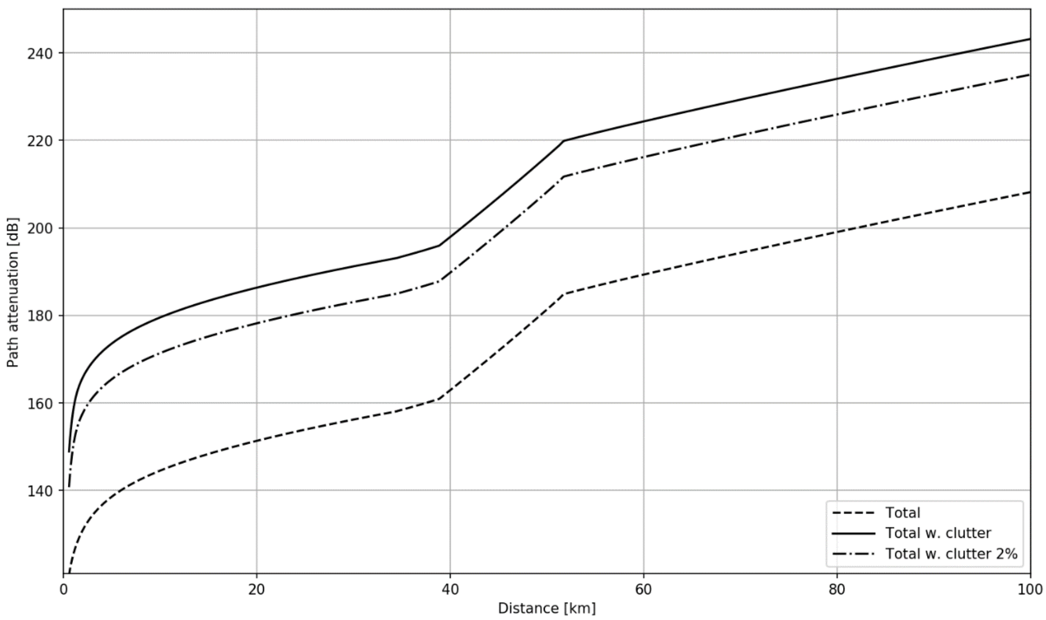

FIGURE A2-6

Path attenuation for BS as a function of distance to the RAS station obtained using Recommendations ITU-R P.452-16 and ITU-R P.2108

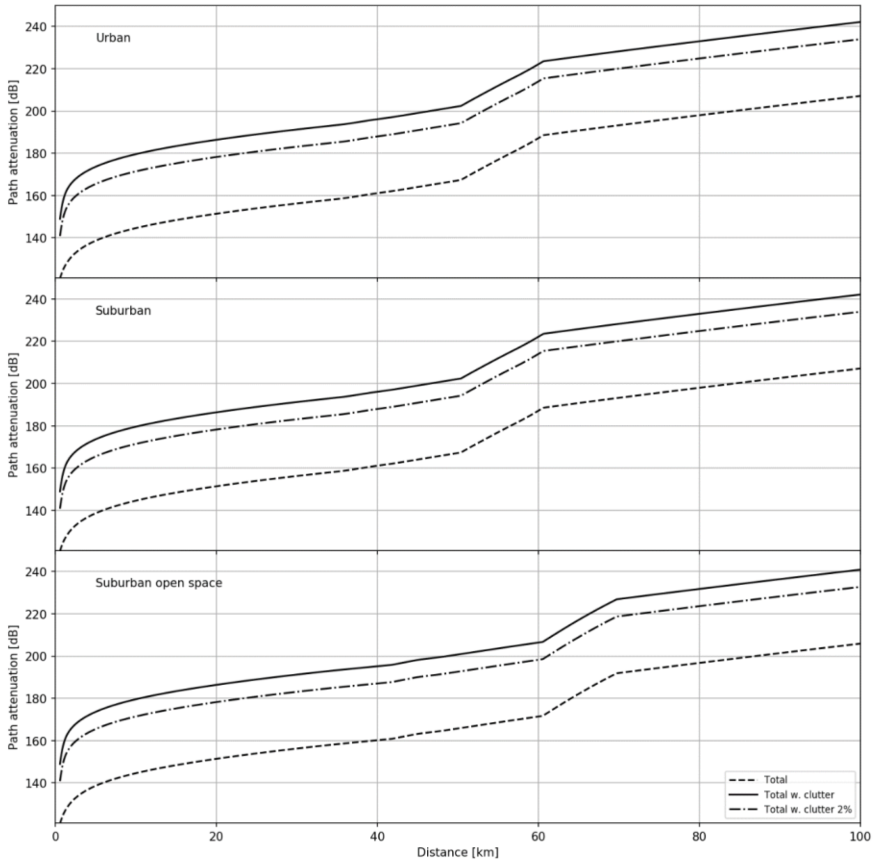

A2.2 Single-interferer scenario

For the single-interferer case, the worst-case situation of a BS or UE device pointing directly towards the RAS station is of main concern.

A2.2.1 Base stations

In the case of BSs, the tilt of the transmitting antenna arrays must be taken into account (−10° or −15° depending on the environmental zone). Using the given antenna patterns (see Figs A2-1 and A2-2), the effective gain towards the RAS station was calculated. Combining this with the total radiated power emitted into the RAS frequency band and the total path attenuation, the power received at the RAS station can be determined. The result is visualized in Figs A2-7 (adjacent frequency band case) and A2-8 (in-band case).

The horizontal dashed red line indicates the Recommendation ITU-R RA.769 power threshold level for detrimental interference. The interception of the received power plots with the dashed red line therefore defines the radius of the coordination zone that would be necessary to protect the RAS station.

FIGURE A2-7

Single-interferer scenario for BS (adjacent-band case)

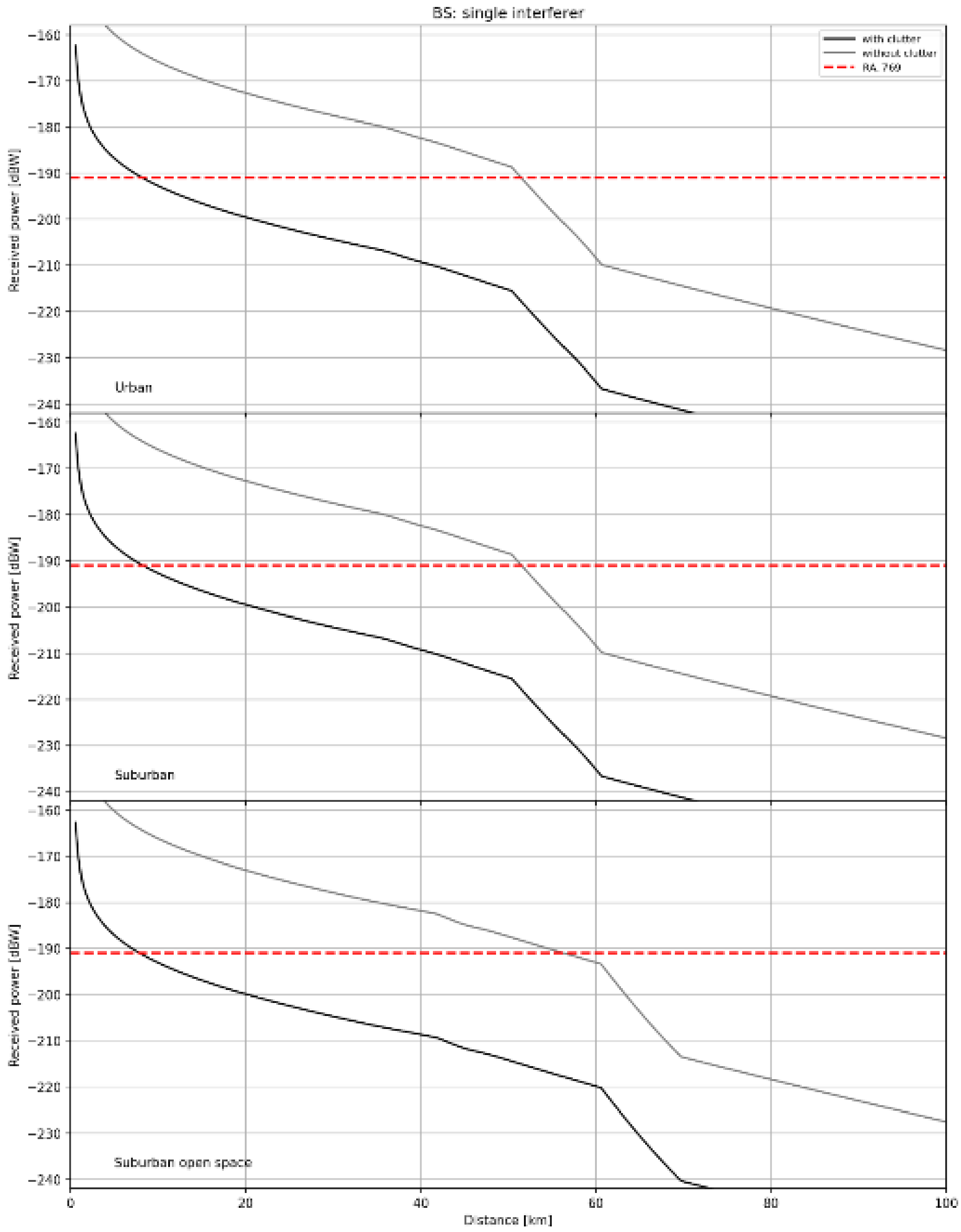

Note to Fig. A2-7: The total received power is displayed as a function of distance to the RAS station for two different transmitter power levels.

FIGURE A2-8

Single-interferer scenario for BS (in-band sharing case)

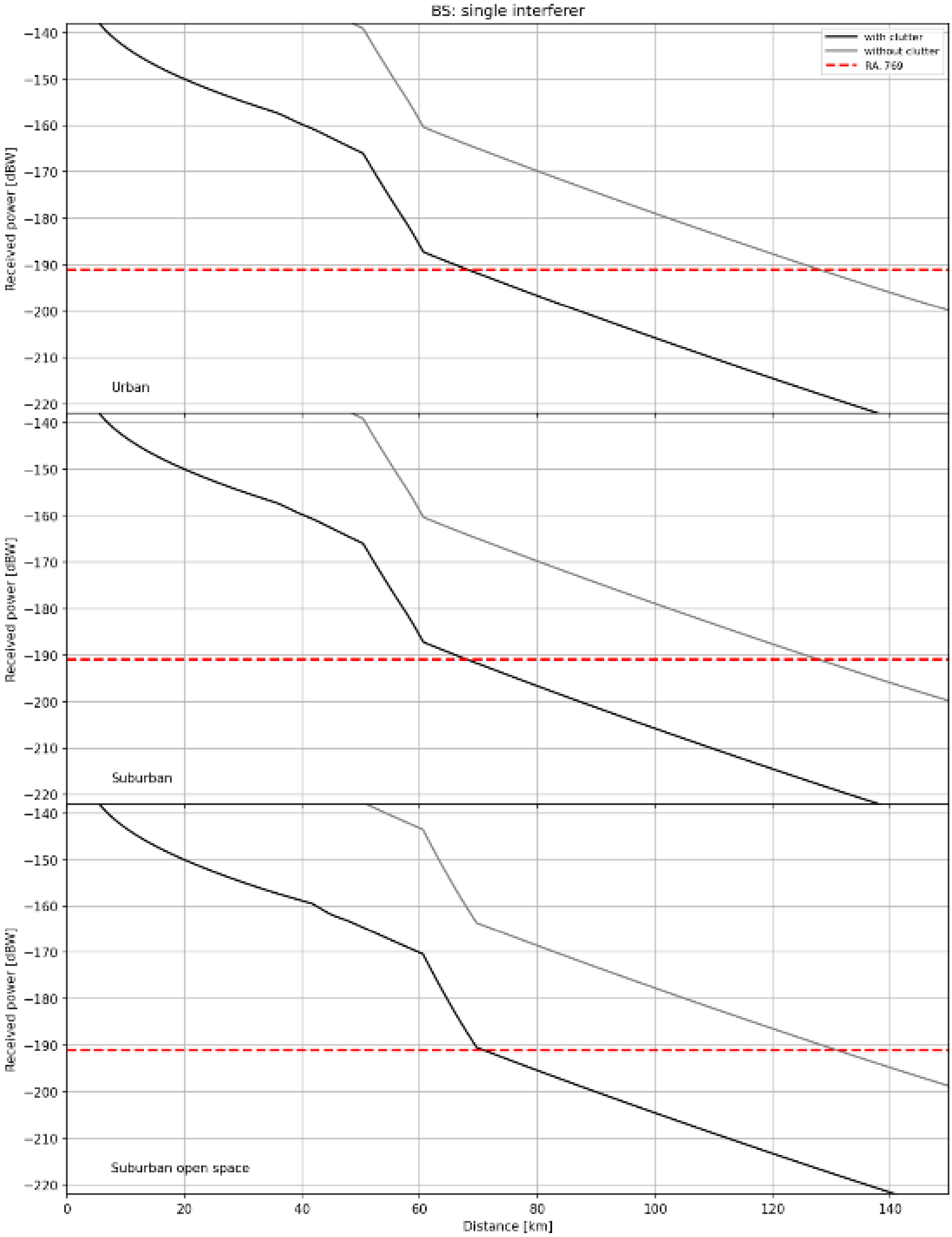

Note to Fig. A2-8: The total received power is displayed as a function of distance to the RAS station.

A2.2.2 User equipment

As for the BS (§ A2.2.1), the single-interferer case was also studied for UE.

Figures A2-9 and A2-10 show the single-interferer received powers obtained for a transmitting antenna tilt of 0 degree.

FIGURE A2-9

Single-interferer scenario for UE (adjacent-band case)

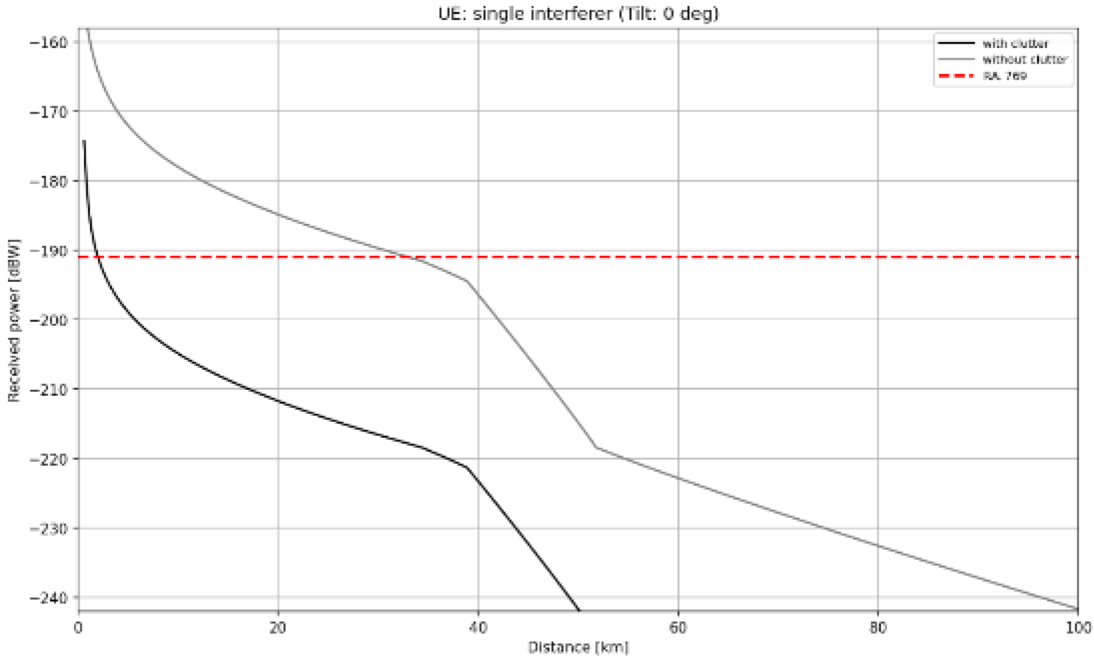

Note to Fig. A2-9: The total received power is displayed as a function of distance to the RAS station for two different transmitter power levels.

FIGURE A2-10

Single-interferer scenario for UE (in-band sharing case)

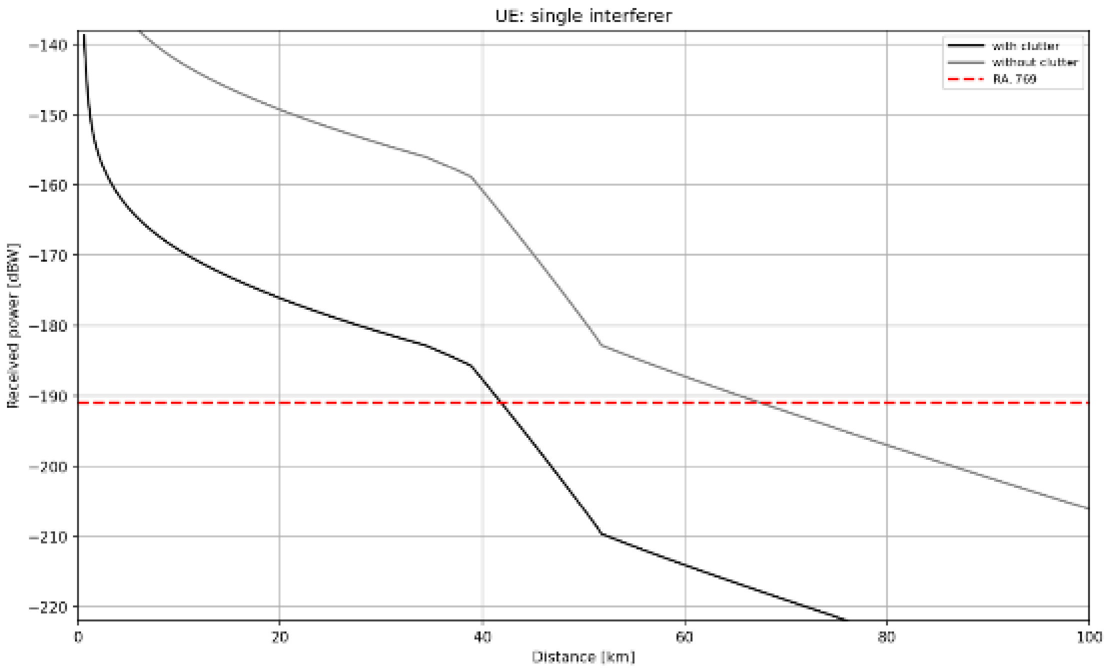

Note to Fig. A2-10: The total received power is displayed as a function of distance to the RAS station.

A2.3 Aggregated power scenario

Not only the single-interferer scenario has to be considered for a compatibility study, but also the aggregate power scenario, which considers the impact of the accumulated emitted power of all IMT devices around an RAS station. Here a Monte Carlo simulation is used to infer the total aggregate power of an ensemble of BS and UE devices, which are located randomly in a box of sufficient size, adhering to the given distribution functions.

A2.3.1 IMT deployment

In Recommendation ITU-R M.2101 several possible deployment topologies are discussed, such as hexagonal or Manhattan-style grid layouts. Typical deployment number densities and other technical parameters were provided in the Chair's Report of TG 5/1 (R15-TG5.1-C-0478).

In the case analysed here, the network topology can be neglected because one needs to average over a very large region such that the aggregate power at the RAS station will be completely defined by the constant deployment densities (per zone type: urban, suburban and suburban open-space hotspot).

Following the Chair's Report of TG 5/1, it is assumed that parameter R_b = 5% (percentage of the considered area which has housing), and that R_a = 7% urban and 3% suburban. For urban zones, up to 30 BSs (or 100 UEs) per km^2 could be present. In suburban zones, the numbers are lower (10 BSs and 30 UEs). There is also the special case of suburban open-space hotspot deployment, with 1 BS and 30 UEs per km^2.

In practice, urban and suburban areas in a region are often clustered. Since no distribution functions for the BS and UE device locations to be used in generic studies were specified in the Chair's Report, a uniform distribution is used here as a reference. Nevertheless, to analyse the impact of clustering effects, the following simple algorithm was developed to produce a typical distribution of urban and suburban zones.

First, a rectangular grid of 400 km × 400 km with cells of size 500 m × 500 m is produced. For each cell a random number is drawn from a normal distribution. The uniform-density generation of urban and suburban cells is possible by computing appropriate percentiles: all cells with a random value above $\left(100\% - \left(R_a^{\text{urban}} + R_a^{\text{suburban}}\right)R_b\right)$ are classified as suburban, while cells with random values above $\left(100\% - R_a^{\text{urban}}R_b\right)$ are classified as urban. The result of this is visualised in Fig. A2-11. To achieve a clustering effect, a correlation length between adjacent pixels must be introduced. This is possible by smoothing the original grid of random numbers with a blurring filter, such as a Gaussian filter. To achieve a realistic effect, three different kernel scales, σ_k, and relative amplitudes were used simultaneously: σ_k = 2 km, 5 km and 15 km with relative amplitudes of 30%, 35%, and 40%. Calculating distribution percentiles of the smoothed random number field leads to the classification of zone types, displayed in Fig. A2-12. The technique is explained in more detail in § A2.3.4.

FIGURE A2-11

Sampling of urban and suburban zones with uniform density; the right panel shows a zoom-in

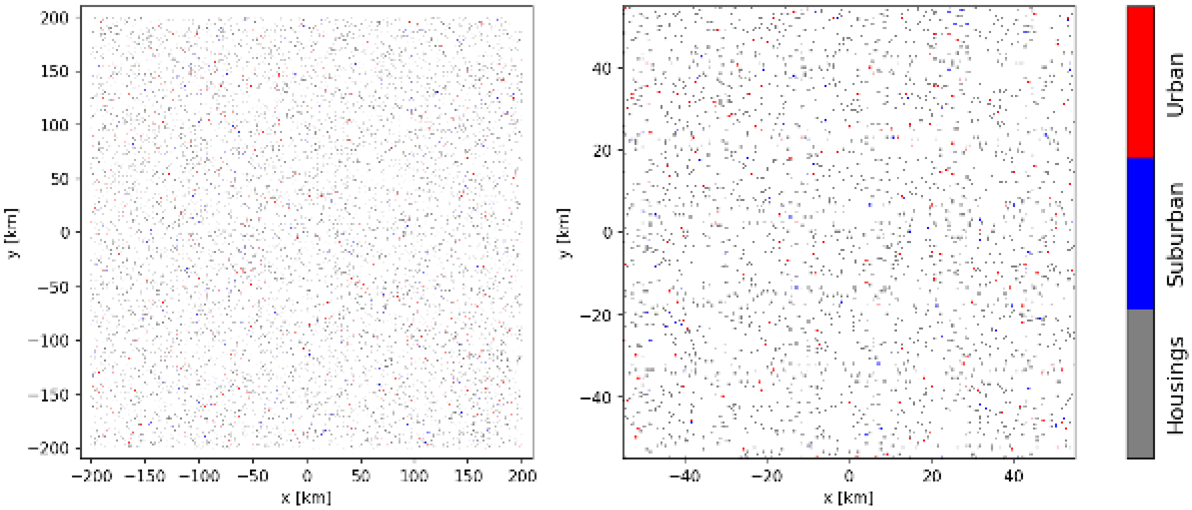

FIGURE A2-12

Sampling of urban and suburban zones with clustering; the right panel shows a zoom-in

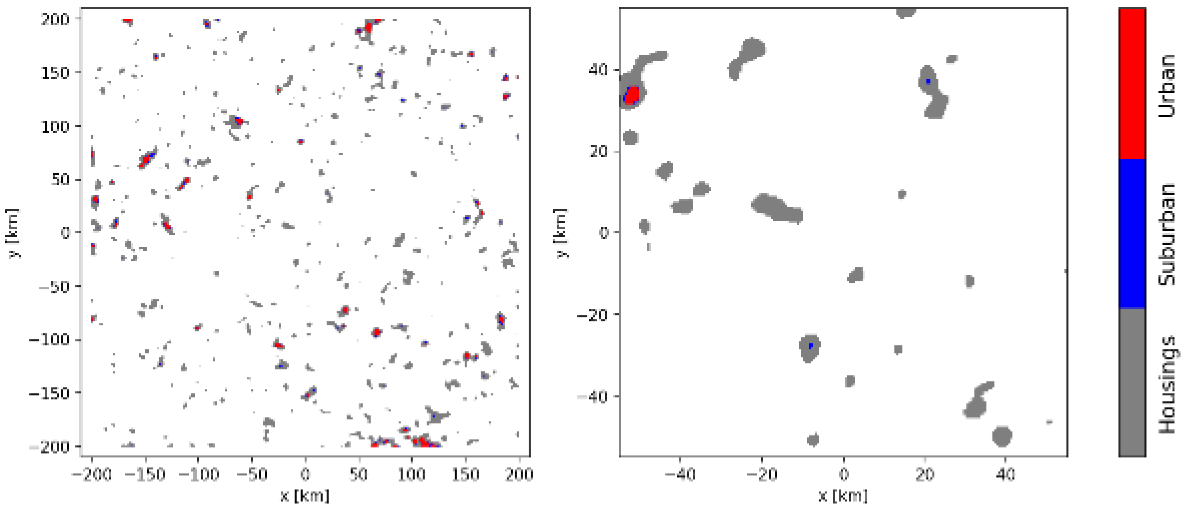

The Monte Carlo methodology used here to calculate the aggregate power is straightforward: BSs are randomly sampled into urban and suburban zones until the total number of devices leads to the specified BS number density. For a box of 400 km × 400 km this leads to 2 400 BSs in suburban, 240 BSs in open-space suburban, and 16 800 BSs in urban zones. To each BS a random azimuthal orientation (bearing) is assigned, and it is assumed that only one sector is active per BS.

From the perspective of a BS, the UE devices are distributed in a forward cone following a radial and angular distribution function as defined in Annex 1 to the TG 5/1 Chair's Report. The distance between BS and UE is given by either a Rayleigh distribution (for urban/suburban; see Table A2-1 for the defining parameters) or a log-normal distribution (for suburban open space). The angular distribution is given by a normal distribution, but with angles restricted within ±60 degrees. The combination of both distributions defines the desired forward cone. The total number of UE devices that are sampled in the box is larger than for BSs: 6 550 (suburban), 650 (suburban open space), and 56 000 (urban).

In addition, a UE device can be rotated almost randomly, with the only restriction that the UE-BS direction be located within ±60° from the antenna normal vector (Annex 1 to the TG 5/1 Chair's Report). More information is also provided in § A1.2.4 to this Report.

A2.3.2 Effective antenna gains and propagation losses

To infer the effective antenna gains of the BS toward the RAS station it is necessary to calculate the directions to the associated UE devices (yielding the Az_i and El_i steering direction of the beam), as well as to the RAS receiver, both in the antenna reference frame. Likewise, for UE gains the direction to the BS and RAS receiver needs to be inferred in the UE antenna frame. This must be determined even for the spurious-domain cases, where the single-element antenna patterns must be used because the UE power control algorithm (see § A2.3.3) is based on the coupling loss between UEs and BSs for which the effective gain of the array-antenna beams must be considered. As the BS and UE antenna frames are rotated and tilted, the calculations are best performed using 3-D vector algebra and appropriate rotation matrices. For the direction to the RAS station, it is furthermore necessary to account for the path propagation horizon angle derived from the propagation loss calculation. The mathematical framework for these calculations is explained in detail in § A1.2.4.

In Fig. A2-13 an example configuration is visualized. Stars and filled circles show positions of BSs and UEs, respectively, whose colours indicate the resulting antenna gain (in dBi) as shown by the colour bar shown in the Figure.

Red lines show the vectors between UEs and their BSs. Black arrows indicate the antenna frame normal vectors, while grey arrows show the direction to the RAS receiver. It is noted that only a projection onto the x-y plane is visualized, although 3-D vectors are used throughout the simulation. As the length of all arrows is equal in 3-D, the apparent length of the arrows in Fig. A2-13 indicates their z-component.

The larger the resulting effective antenna gain towards the RAS station, the closer the vector between UE and BS (red lines) aligns with the vector to the receiver (grey arrows). The orientation of the transmitting antenna arrays (black arrows) also plays a role because it changes the side-lobes of the formed beam. For example, a rotation about the forward direction (defined by the antenna normal vector) will only mildly change the forward gain, but can have significant impact on the gain into any other direction.

One detail which must be considered to calculate the BS gain for the composite-array scenario is that one BS often serves multiple UEs. In such cases, the effective BS gain is determined by averaging over the individual gains resulting from the beam pointing to the various UE devices.

The propagation losses can simply be derived from the Recommendation ITU-R P.452-16 prediction over the distance given from the respective grid cell to the map centre (where the RAS station is situated). As discussed in § A2.1.3, the clutter losses are calculated by assigning a random value to p_L (uniformly distributed over the range 0% to 100%). For comparison, a version of the simulation was also run without clutter losses.

FIGURE A2-13

Example of a BS-UE configuration

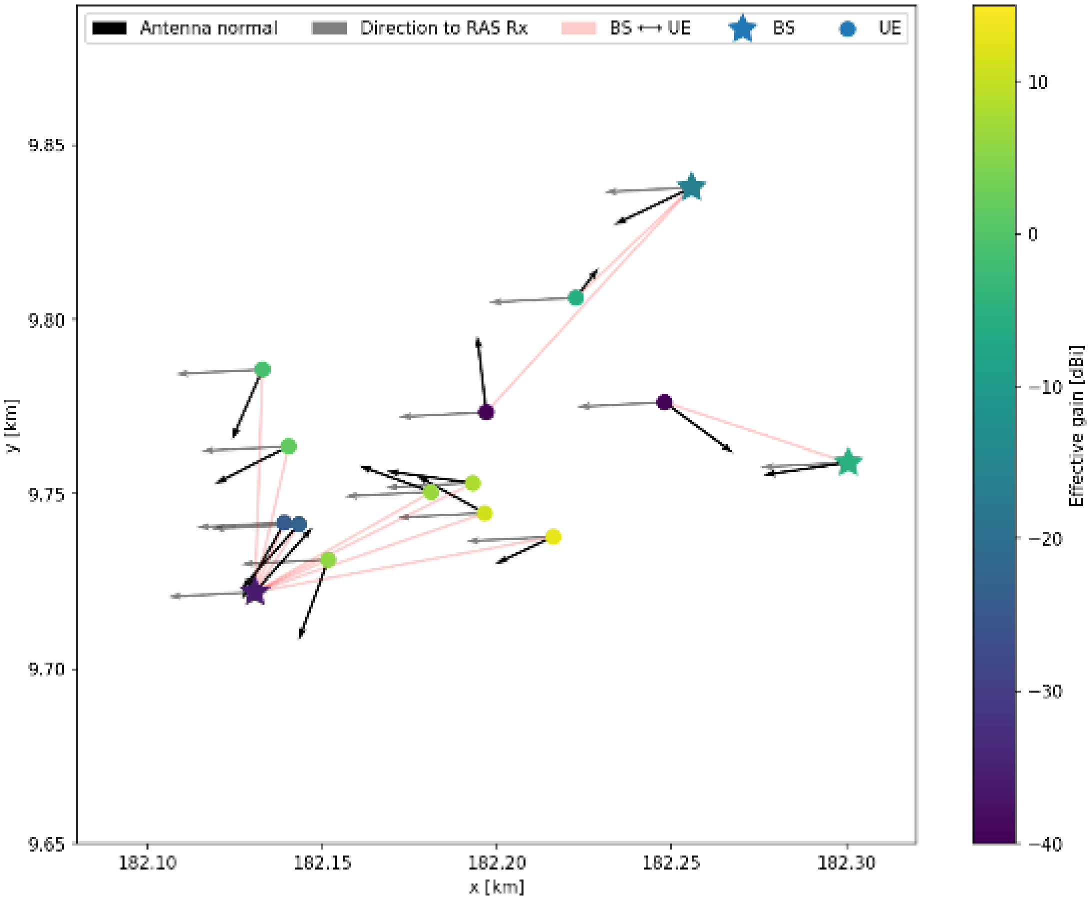

A2.3.3 UE power control

IMT-2020 UE will be subject to power control. Depending on the distance of each UE device and path type (Line of Sight, Non-Line-of-Sight) its output power can be increased or decreased for efficient use of power consumption. Furthermore, the number of other active devices in the vicinity plays a role in the power control algorithm, which is described in Recommendation ITU-R M.2101. The path propagation loss between UEs and their associated BSs is calculated according to the equations given in 3GPP TR 38.901 (Umi – Street Canyon scenario). For the power control algorithm, the coupling loss must be applied, which is the path propagation loss combined with the effective gains of the formed beams at the UE device and BS. In Fig. A2-14, the effect of the power control on the UE output levels is visualised: the UE devices are now coloured according to the difference (in dB) in output power after the power control algorithm is applied with respect to the nominal output power. For most UEs the output power will be lower than nominal, but for distant (or Non-LoS) devices the output could be up to 12 dB higher than nominal.

FIGURE A2-14

Effect of UE power control for the example configuration shown in Fig. A2-13 – difference (in dB) in output power after application of the power control algorithm

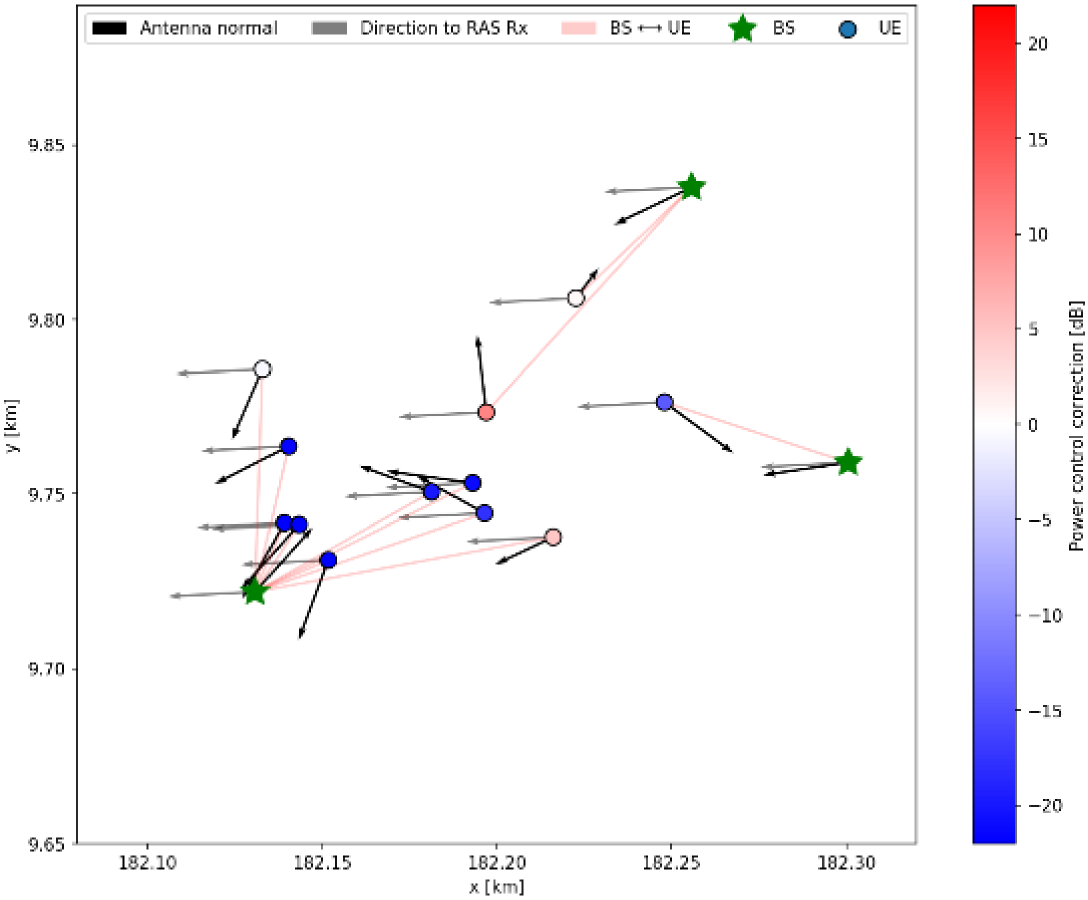

A2.3.4 Aggregated power at the RAS receiver

Each Monte Carlo iteration (i.e. one realization of a BS+UE configuration within the box) yields a total power level received at the RAS station, which is calculated by simply aggregating all individually emitted power levels and accounting for antenna gains and propagation losses. In practice, in effectively all cases the RAS interference threshold levels are exceeded.

A minimal separation distance can be calculated by determining the received power as a function of an exclusion-zone radius, R_i. For each R_i the total contribution of devices outside a circular zone of radius R_i is inferred. As this is performed for each iteration, an ensemble of curves (received power as a function of separation distance) is generated. By studying the distribution percentiles, the 50% (median) or highest 2% curve can be extracted. The latter matches the highest acceptable data loss for the RAS, following Recommendation ITU-R RA.1513. The minimal separation distances are defined by the crossing points of the received-power curves, with the threshold power level for detrimental interference given in Recommendation ITU-R RA.769.

For each of the two deployment scenarios (uniform-density and clustered), as well as for the spurious (adjacent) and in-band domain, a Monte Carlo simulation was run. The spurious-domain case calculation is somewhat less complex because no composite beam patterns must be taken into account, only the single element patterns. The ensemble curves and distribution percentiles are displayed for the various scenarios in Figs A2-15 through A2-18.

FIGURE A2-15

Aggregate power (adjacent-band case, uniform density) as a function of separation distance

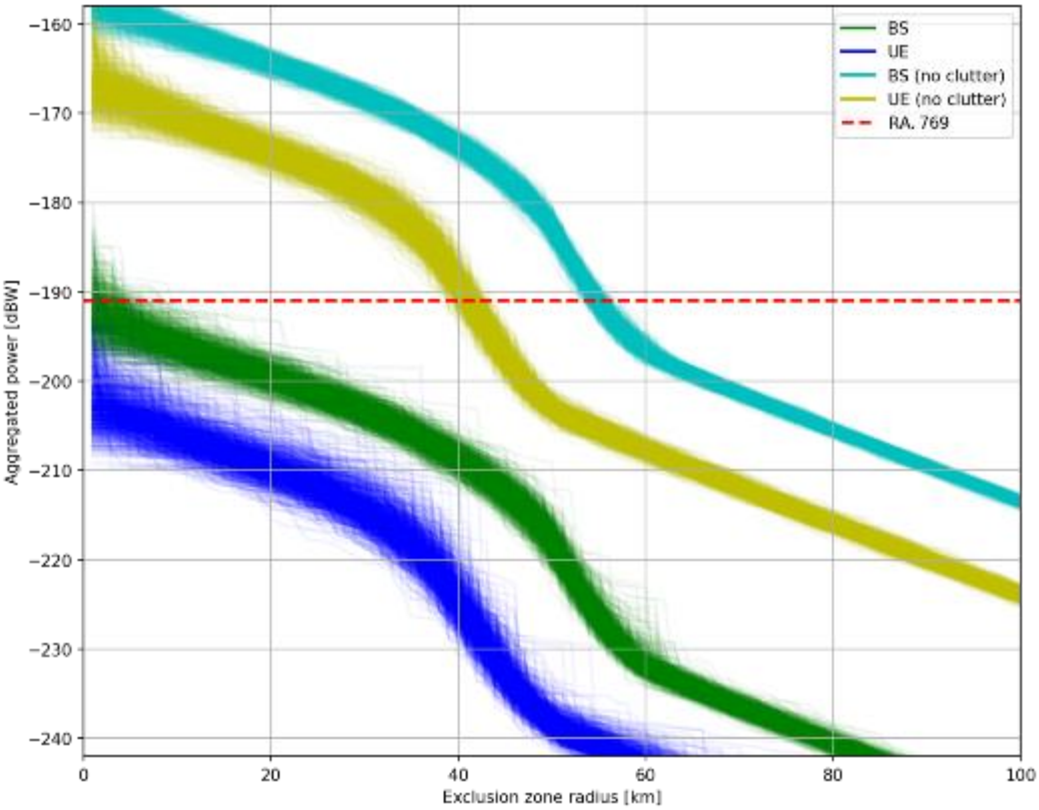

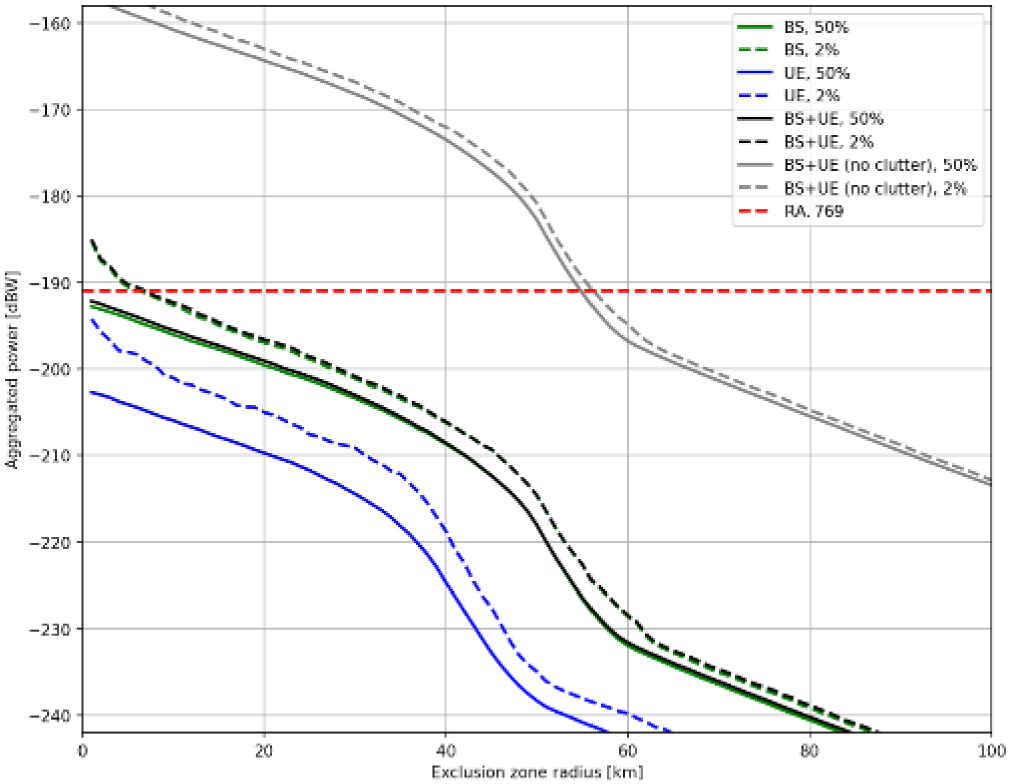

FIGURE A2-16

Aggregate power (adjacent-band case, clustered) as a function of separation distance

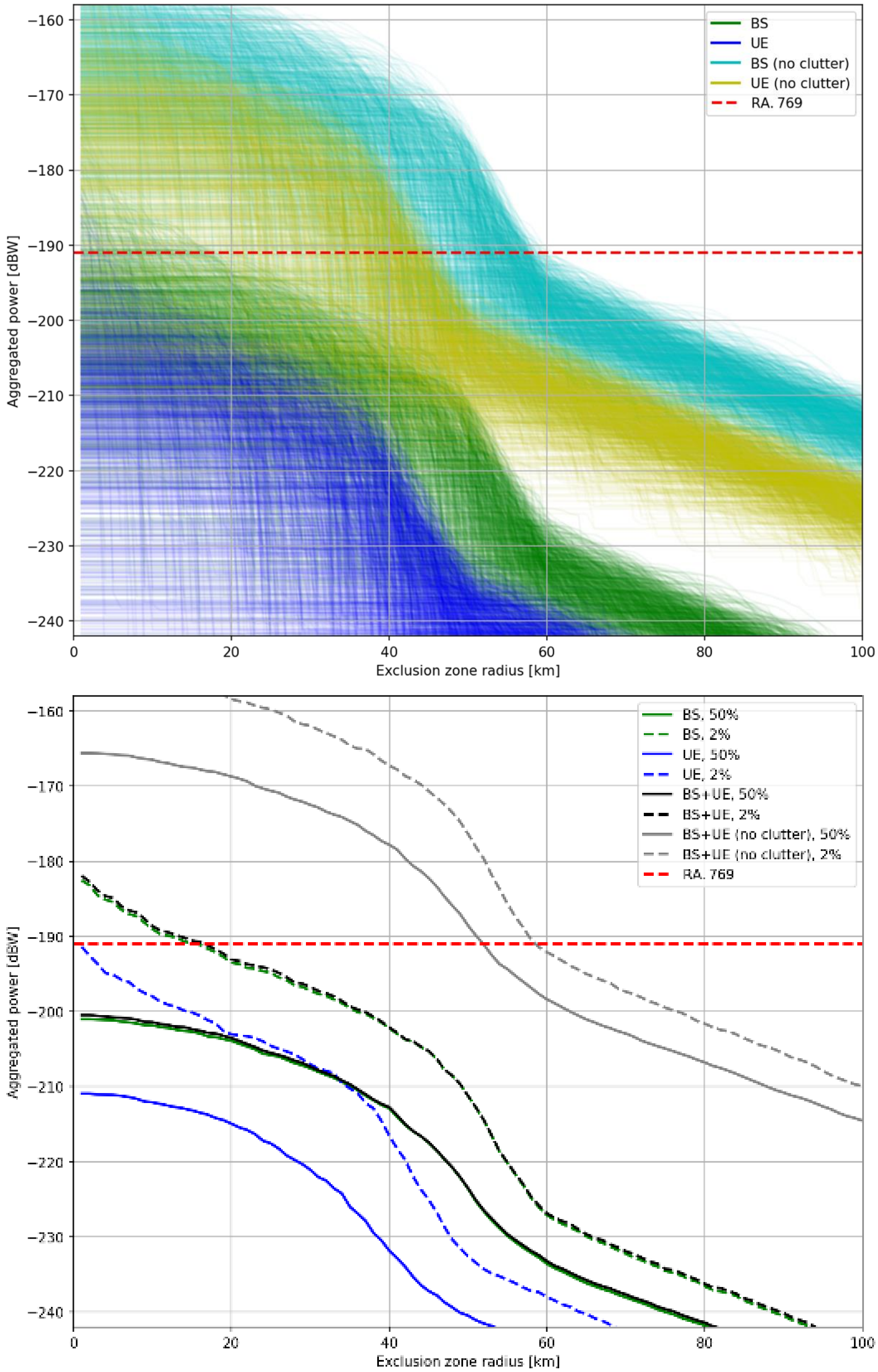

FIGURE A2-17

Aggregate power (in-band case, uniform density) as a function of separation distance

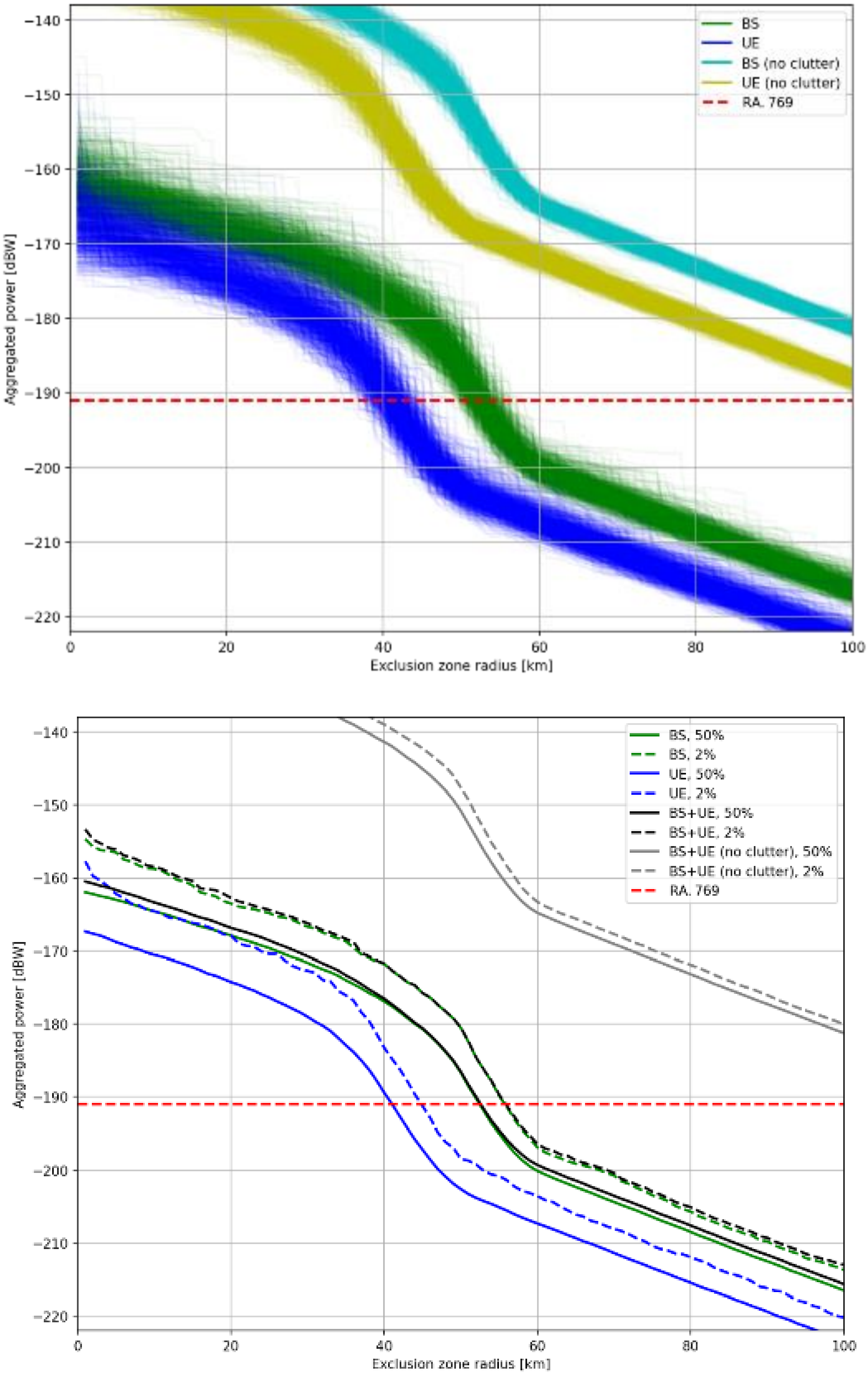

FIGURE A2-18

Aggregate power (in-band case, clustered) as a function of separation distance

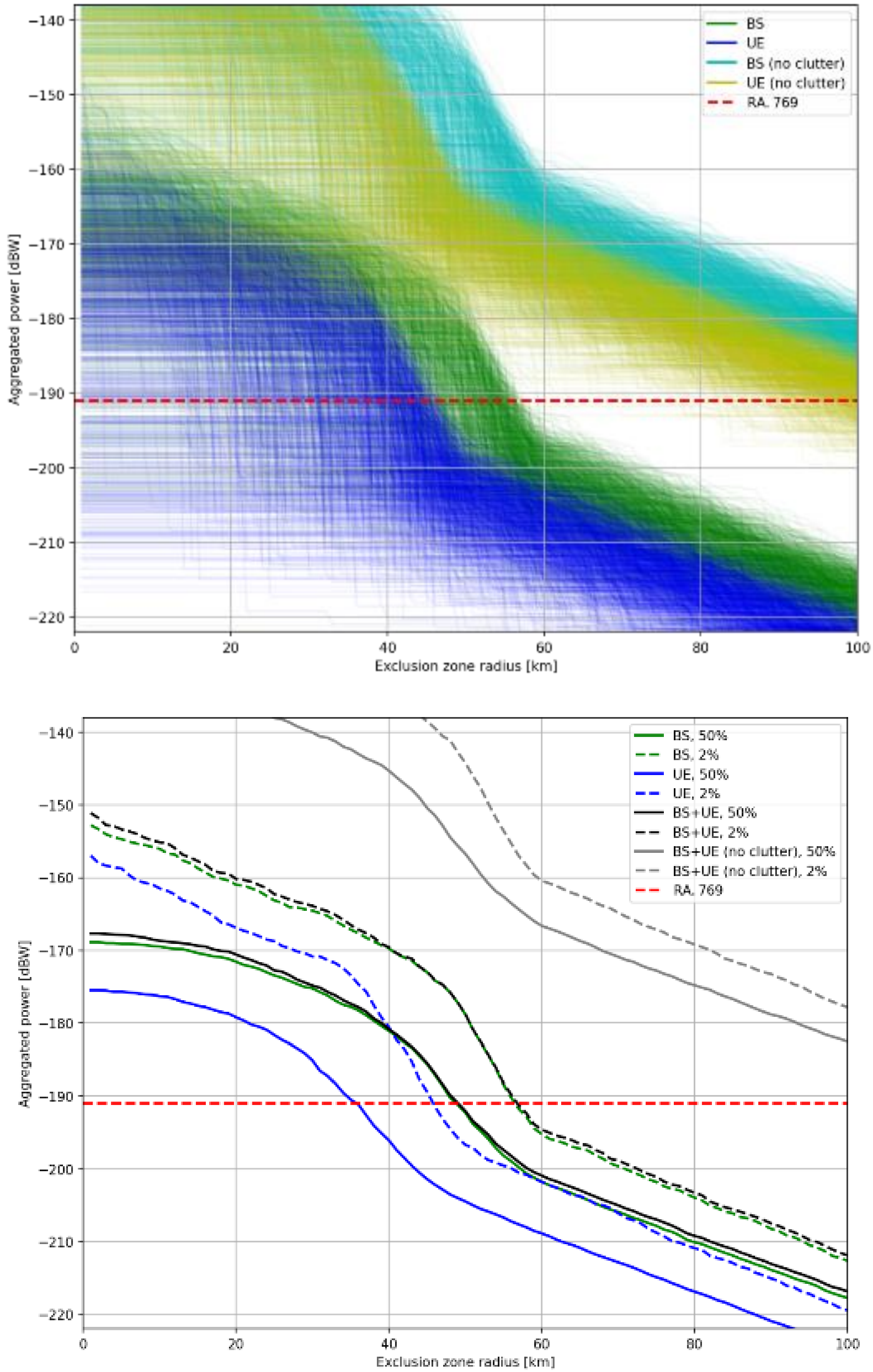

A2.4 Results

A2.4.1 Adjacent-band case (spurious domain)

For the generic compatibility study between the RAS in the frequency band 42.5-43.5 GHz and IMT systems in the adjacent frequency band 40.5-42.5 GHz, it was assumed that a guard band between the IMT frequency band and the RAS frequency band will be implemented such that the RAS will be affected in the spurious domain of the emission mask of the IMT devices, only. Both single-interferer and aggregate emission scenarios were studied.

Results are listed in Table A2-2 as separation distances, or coordination zone radii, around the RAS station. It must be noted that the clutter model in Recommendation ITU-R P.2108, § 3.2, which was used for this study, is only appropriate for urban and suburban land cover types and only if the IMT devices are below the rooftops of the housings. In some countries, these conditions may not be fulfilled when assignments are made. Therefore, to allow for comparison and to indicate the impact of the clutter, results are also provided for zero-clutter losses.

For spurious emissions of IMT systems, a regulatory limit for the total radiated spectral power of −30 dB(m/MHz) was set at WRC-19. For a generic flat-terrain aggregation scenario with uniform deployment of BSs, separation distances of 7 km are required (BS-only: 7 km, UE-only: 1 km). If no clutter would apply, this distance rises to 57 km, which demonstrates the enormous impact of the clutter environment on the results. The single-interferer study was laid out as worst-case scenario. The results are comparable with the ones from the aggregation scenario.

TABLE A2-2

Separation distances from RAS stations for various scenarios in the adjacent-band case

Zone	With clutter	BS (km)	UE (km)	BS+UE (km)
Single interferer				
Urban	Yes	8	2	n/a
Suburban	Yes	8	2	n/a
Suburban open space	Yes	8	2	n/a
Urban	No	52	33	n/a
Suburban	No	52	33	n/a
Suburban open space	No	56	33	n/a
Aggregate scenario, uniform density (2% / 50%)				
	Yes	7 / 1	1 / 1	7 / 1
	No	57 / 55	44 / 42	57 / 55
Aggregate scenario, clustered density (2% / 50%)				
	Yes	16 / 1	1 / 1	17 / 1
	No	59 / 52	46 / 37	59 / 52

A2.4.2 In-band (sharing) case

The in-band sharing case concerns RAS and IMT systems both operating in the frequency band 42.5-43.5 GHz. The resulting separation distances are listed in Table A2-3.

The necessary separation distances are, as expected, larger than in the adjacent-band case. For the aggregation scenario with uniform deployment of BSs, separation distances of 56 km are required (BS-only: 56 km, UE-only: 45 km). If no clutter would apply, this distance rises to more than 100 km. The exact figure cannot be determined without increasing the simulation box significantly. The single-interferer separation distances for BS are slightly larger than for the aggregation scenario owing to the large maximum antenna gain of AAS.

TABLE A2-3

Separation distances from RAS stations for various scenarios in the in-band sharing case

Zone	With clutter	BS (km)	UE (km)	BS+UE (km)
Single interferer				
Urban	Yes	68	42	n/a
Suburban	Yes	68	42	n/a
Suburban open space	Yes	71	42	n/a
Urban	No	128	68	n/a
Suburban	No	128	68	n/a
Suburban open space	No	131	68	n/a
Aggregate scenario, uniform density (2% / 50%)				
	Yes	56 / 53	45 / 41	56 / 53
	No	>100	>100	>100
Aggregate scenario, clustered density (2% / 50%)				
	Yes	57 / 49	47 / 37	57 / 50
	No	>100	>100	>100

Annex 3
(informative)

Sharing and compatibility studies conducted by Japan between RAS operating in the band 42.5-43.5 GHz and IMT systems operating around 42.5 GHz

A3.1 Introduction

In the frequency allocation plan of the Ministry of Internal Affairs and Communications of Japan, the frequency band 42.5-43.5 GHz is allocated to the RAS, and some RAS observatories in Japan are designated for protection on the basis of the Radio Law of Japan and the notification of the Ministry of Internal Affairs and Communications. Sharing and compatibility studies between three RAS observatories and IMT systems were conducted.

A3.2 Sharing and compatibility studies between a RAS station and IMT BSs

The results of the sharing and compatibility studies of between the RAS observatories and the BSs of the IMT system at the same and in adjacent bands are shown below.

A3.2.1 Parameters used in the sharing and compatibility studies

Table A3-1 shows the parameters of the RAS observatories used in the studies.

TABLE A3-1

Parameters for the RAS stations

Parameters	Values	Remarks
Name / antenna height	VERA Mizusawa / 15 m Nobeyama 45-m / 27.5 m VERA Iriki / 15 m	Assumed values for the antenna heights
Receiving frequency	42.5 GHz	
Maximum gain	0 dBi	
Antenna directivity	Omni-directional	
Threshold interference power based on the protection criterion	−191 dBW/1 000 MHz = −191 m/MHz, 2% of fraction of time	Continuum mode in Rec. ITU-R RA.769

Table A3-2 shows the parameters of the IMT BSs used in the studies.

TABLE A3-2

Parameters for the IMT BSs

Parameters	Values	Remarks
Transmitting frequency	42.5 GHz	
Transmitting power	3 dBm/MHz	For studies in the same band
Unwanted emission	−13 dBm/MHz	For studies in adjacent band
Antenna height	6 m	
Antenna directivity	Taken from Rec. ITU-R M.2101	Averaged and maximum patterns
Maximum gain	~26 dBi	5 dBi per element, 8 × 16 elements
Mechanical tilt	10 degrees	

The interference power was modelled using antenna directivity, shown in Figs A3-1 and A3-2, in order to consider the influence of fluctuations in antenna directivity due to the application of beamforming at the IMT BSs. Figure A3-1 shows the average values of antenna directivity characteristics of the IMT BS beamforming according to the location of the IMT mobile stations, modelled as averaged antenna gain values in any direction after statistical processing using a large number of snapshots). Alternatively, in Fig. A3-2, after the same statistical processing, maximum values of the antenna gain were modelled in an arbitrary direction (maximum pattern).

FIGURE A3-1

Antenna directivity of the IMT BS (averaged pattern)

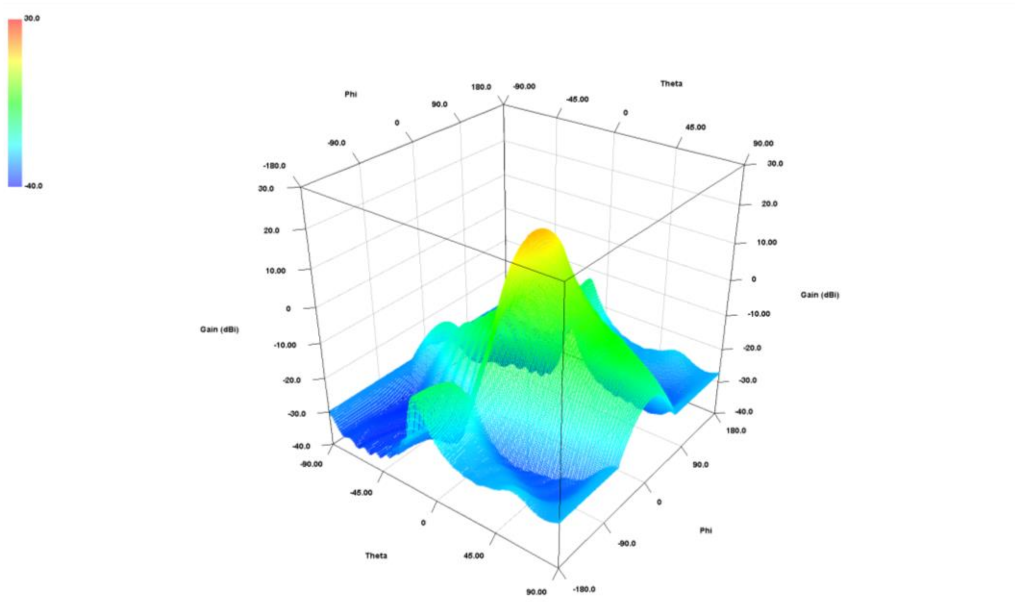

FIGURE A3-2

Antenna directivity of the IMT BS (maximum pattern)

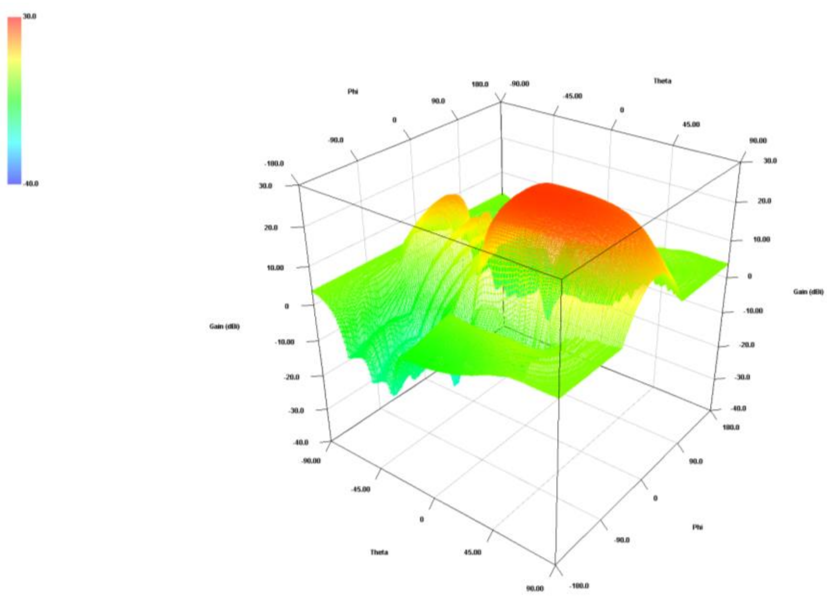

The conditions shown in Table A3-3 were used for the propagation model and various settings of the location of IMT BSs in the studies.

TABLE A3-3

Other conditions used for the studies

Item	Content
Propagation model	Recommendation ITU-R P.452 with 2% of fraction of time
Locations of IMT BSs potentially installed	1 IMT BS in a mesh (500 m × 500 m)

The aggregate interference from multiple IMT BSs to the RAS observatories was also evaluated according to the procedure shown in Table A3-4, assuming that the IMT BSs will be installed sequentially at points in accordance with the daytime population in a mesh over the pre-determined area around each of the RAS observatories.

TABLE A3-4

Evaluation flow chart when taking aggregate interference into account

(1)	Select meshes in the order of largest daytime population within the mesh.
(2)	In the mesh selected in (1), calculate the interference power using the maximum pattern values for the antenna directivity of the IMT BSs (Note 1).
(3)	If the calculated interference power is below the threshold value, the IMT BS is installed in the mesh and proceed to (4). If it is above the threshold value, it is impossible to install an IMT BS in the mesh, and return to (1).
(4)	For the mesh where the IMT BS can be installed in (3), calculate the interference power using the average pattern values for antenna directivity of the BSs (Note 2), and proceed to (5).
(5)	To calculate aggregate interference power, accumulate the interference power calculated in (4) for the mesh on which the IMT BSs can be installed so far. If the calculated aggregate interference power is below the threshold interference power of the RAS observatories, return to (1). If the calculated value exceeds the threshold interference power, record the number of IMT BSs up to just below the excess as the number of stations that can be installed, and record the difference between the threshold interference power and the aggregate interference power just below the excess as an interference margin. This completes the calculation.

NOTE 1 – Judgment is based on the interference power calculated with the maximum pattern values, considering the possibility of the instantaneous interference from one BS affecting.

NOTE 2 – As the interference from multiple IMT BSs is assumed not to be exerted in the maximum pattern at the same timing, the interference power is calculated with the average pattern values and accumulated.

A3.2.2 Study results between the IMT BSs and the VERA Mizusawa station

The interference power received at the VERA Mizusawa station from the IMT BSs was evaluated. The points to install IMT BSs were selected based on the daytime population in the Hokkaido and Tohoku areas (northern part of Japan). Figure A3-3 shows the location of the points where the IMT BSs are potentially installed (green, in total of 5 511 points) and the location of the RAS observatory (red).

FIGURE A3-3

Locations of the RAS observatory (Red) and the IMT BSs (Green)

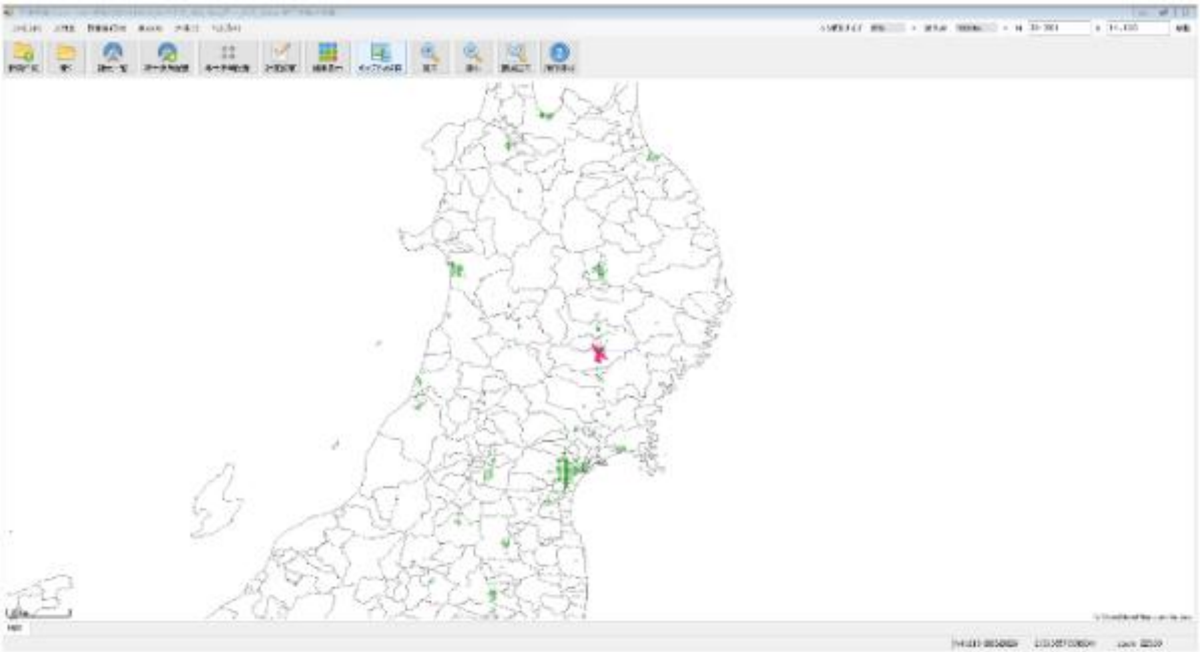

Figure A3-4 shows the results of evaluating the magnitude of the interference power to the VERA Mizusawa station from the individual IMT BSs at each location depending on the distance from the RAS observatory. In this Figure, a blue plot shows the magnitude of the interference power from one IMT BS, and the red horizontal line shows the threshold interference power (within the band) at the RAS observatory. The averaged antenna pattern of the IMT BS was used in evaluating interference power (see Fig. A3-1).

From this Figure, the magnitude of the interference power from the IMT BSs satisfies the threshold interference power at the RAS observatory under the in-band interference condition if a separation distance of approximately 35 km or more is secured. In addition, under the condition of adjacent-band interference, the threshold interference power at the RAS observatory is satisfied if a separation distance of approximately 30 km or more is secured. Even under the above-mentioned conditions within the separation distance, threshold interference power of the RAS observatory may be satisfied in some cases depending on the location of the IMT BS, the terrain existing on the propagation path to the RAS observatory, or the shielding condition from buildings.

Table A3-5 shows the results of calculating the number of IMT BSs that can be installed when aggregate interference is taken into consideration. Threshold values of −201 dBm/MHz and −211 dBm/MHz were set for determining whether to install an IMT BS at each point, considering 5 111 points in the Tohoku and Hokkaido areas based on the daytime population. These threshold values are adopted as 10 dB and 20 dB, respectively, which is lower than the threshold interference power (i.e. the protection criterion) at the RAS observatory. The interference margin in this table gives the difference between the cumulative interference power (aggregate interference power) from multiple IMT BSs and the threshold interference power at the RAS observatory when the maximum installable number of IMT BSs are installed.

Table A3-5 shows that about 5 000 or more IMT BSs satisfying the threshold interference power at the RAS observatory can be installed in the Tohoku and Hokkaido areas if the threshold value of the interference power that determines whether to install the BS is set appropriately.

FIGURE A3-4

Received interference power at the VERA Mizusawa station from IMT BSs

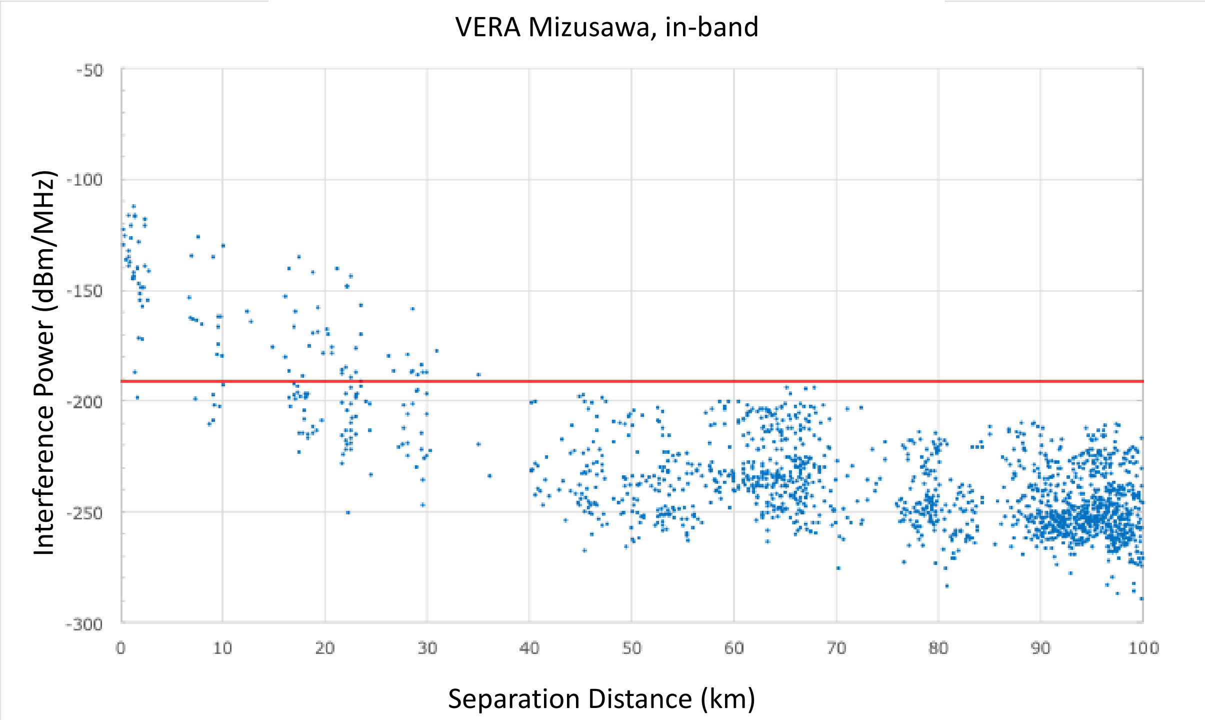

a) In-band interference

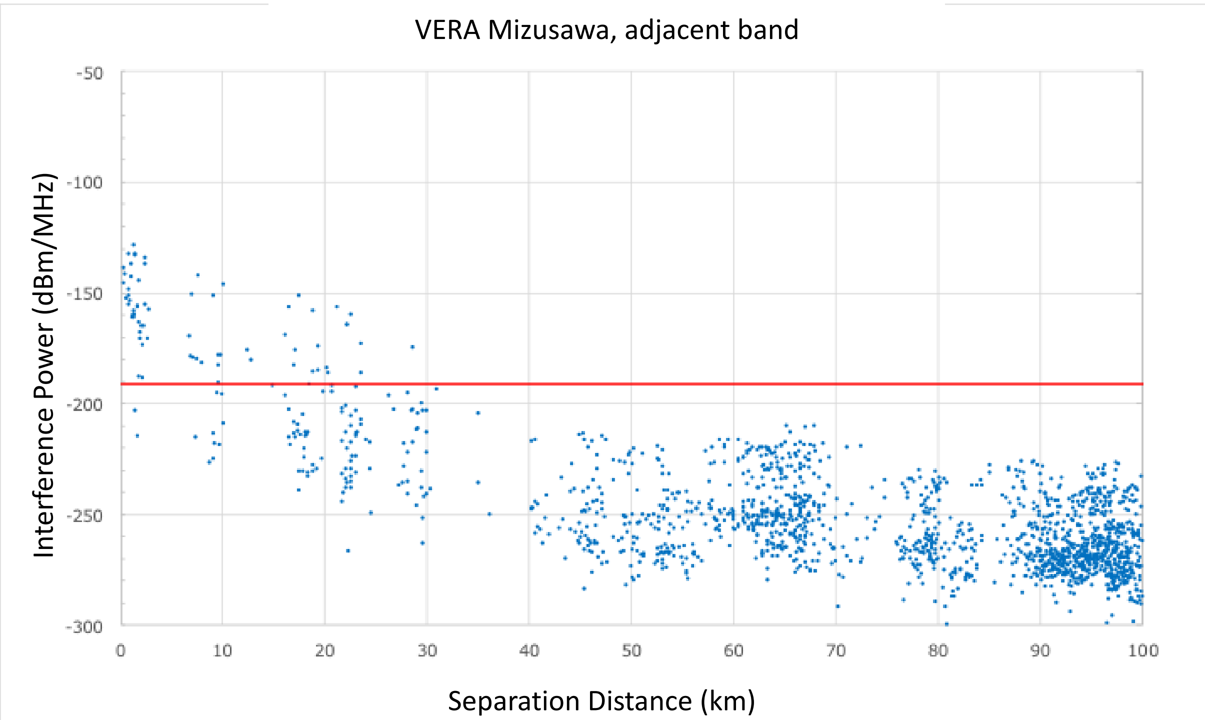

b) Adjacent-band interference

TABLE A3-5

Maximum installable number of IMT BSs for the aggregate interference case

(a) In-band case		
Interference threshold value (dBm/MHz)	−201	−211
Maximum installable number of IMT BSs	5 192	4 944
Number of points where IMT BSs are not installable	319	567
Interference margin (dB)	6.5	14.9
(b) Adjacent-band case		
Maximum installable number of IMT BSs	5 372	5 264
Number of points where IMT BSs are not installable	139	247
Interference margin (dB)	9.0	18.2

A3.2.3 Study results between the IMT BSs and the Nobeyama 45-m Telescope

The interference power received at the Nobeyama 45-m Radio Telescope from the IMT BSs was evaluated. The points to install IMT BSs were selected based on the daytime population in the Kanto, Chubu, and Hokuriku areas (central Japan). Figure A3-5 shows the locations where the IMT BSs are potentially installed (green, in total of 23 253 points) around the RAS observatory (red).

FIGURE A3-5

Locations of the RAS observatory (Red) and the IMT BSs (Green)

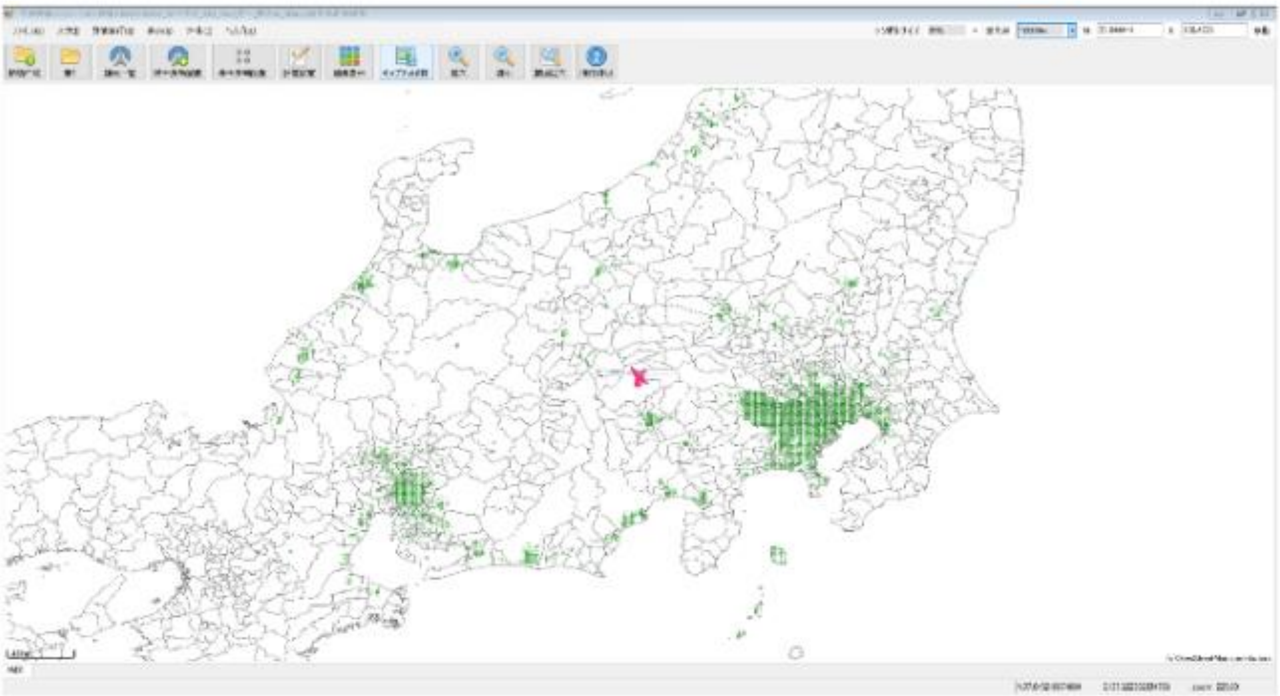

Figure A3-6 shows the results of evaluating the magnitude of the interference power to the Nobeyama 45-m Radio Telescope from the individual BSs at each location depending on the distance from the RAS observatory. In this Figure, a blue plot shows the magnitude of the interference power from each IMT BS, and the red horizontal line shows the threshold interference power (within the band) at the

RAS observatory. The averaged antenna pattern of the IMT BS was used in evaluating interference power (see Fig. A3-1).

From this Figure, one point that exceeds the threshold interference power at the RAS observatory with a separation distance of about 42 km under the in-band interference condition can be found, but all other IMT BS points satisfy the threshold interference power at the RAS observatory.

Table A3-6 shows the calculation results of the number of installable IMT BSs when aggregate interference is taken into consideration. Threshold values of −201 dBm/MHz and −211 dBm/MHz were set for determining whether to install an IMT BS at each point, considering 23 253 points in Kanto, Chubu, and Hokuriku regions based on the daytime population. These threshold values are adopted as 10 dB and 20 dB, respectively, lower than the threshold interference power (i.e. protection criterion) at the RAS observatory. The interference margin in this Table gives the difference between the cumulative interference power (aggregate interference power) from multiple IMT BSs and the threshold interference power at the RAS observatory when the maximum installable number of BSs are installed.

Table A3-6 shows that more than 20 000 BSs satisfying the allowable interference power of the RAS observatory can be installed in Kanto, Chubu, and Hokuriku regions if the threshold value of the interference power that determines whether to install an IMT BS is set appropriately.

FIGURE A3-6

Received interference power at the Nobeyama 45-m Telescope from IMT BSs

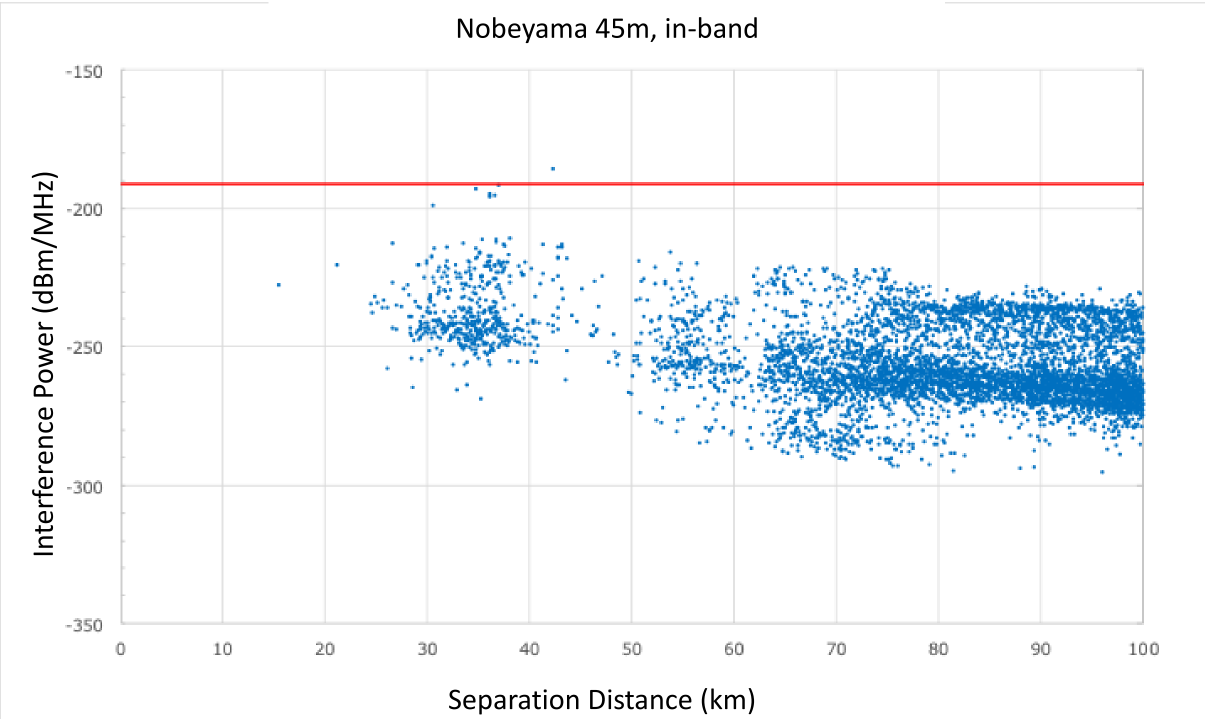

a) In-band interference

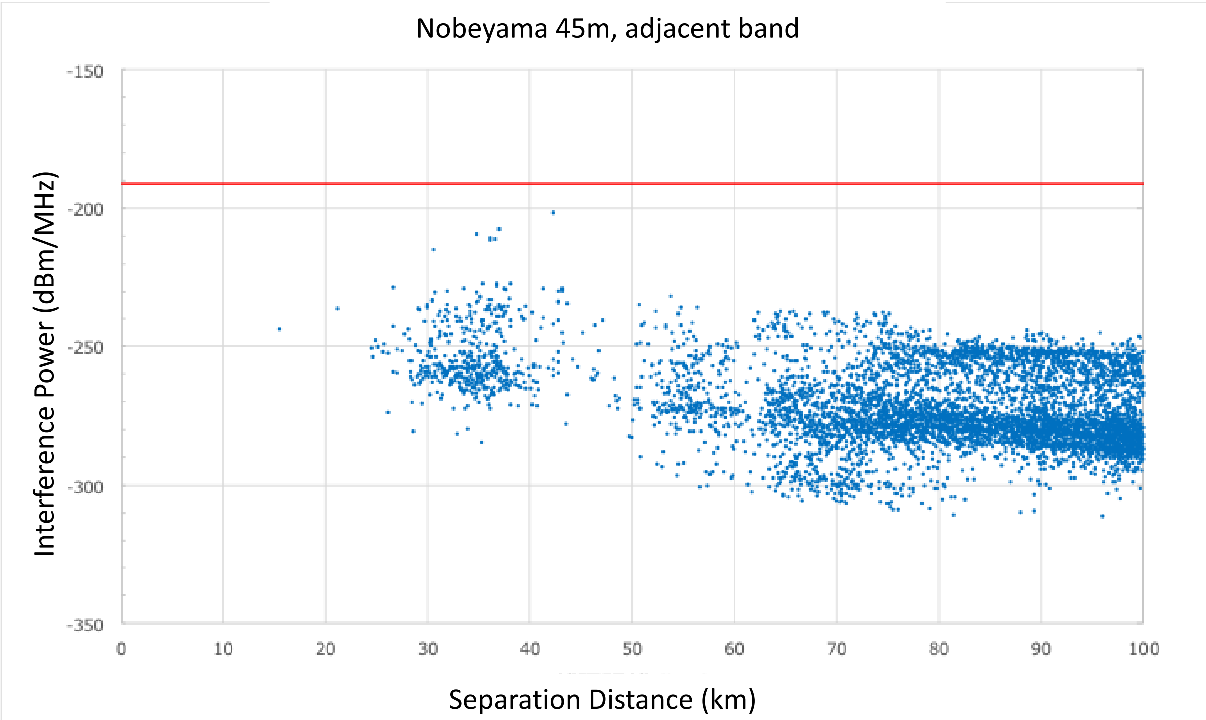

b) Adjacent-band interference

TABLE A3-6

Maximum installable number of IMT BSs for the aggregate interference case

(a) In-band case		
Interference threshold value (dBm/MHz)	−201	−211
Maximum installable number of IMT BSs	23 215	23 035
Number of points where IMT BSs are not installable	38	218
Interference margin (dB)	7.6	12.0
(b) Adjacent-band case		
Maximum installable number of IMT BSs	23 246	23 248
Number of points where IMT BSs are not installable	7	5
Interference margin (dB)	24.9	36.1

A3.2.4 Study results between the IMT BSs and the VERA Iriki station

The interference power received at the VERA Iriki station from the IMT BSs was evaluated. The points to install IMT BSs were selected based on the daytime population in the Kyushu area (south-western Japan). Figure A3-7 shows the location of points where the IMT BSs are potentially installed (green, in total of 6 009 points) around the RAS observatory (red).

FIGURE A3-7

Locations of the RAS observatory (red) and the IMT BSs (green)

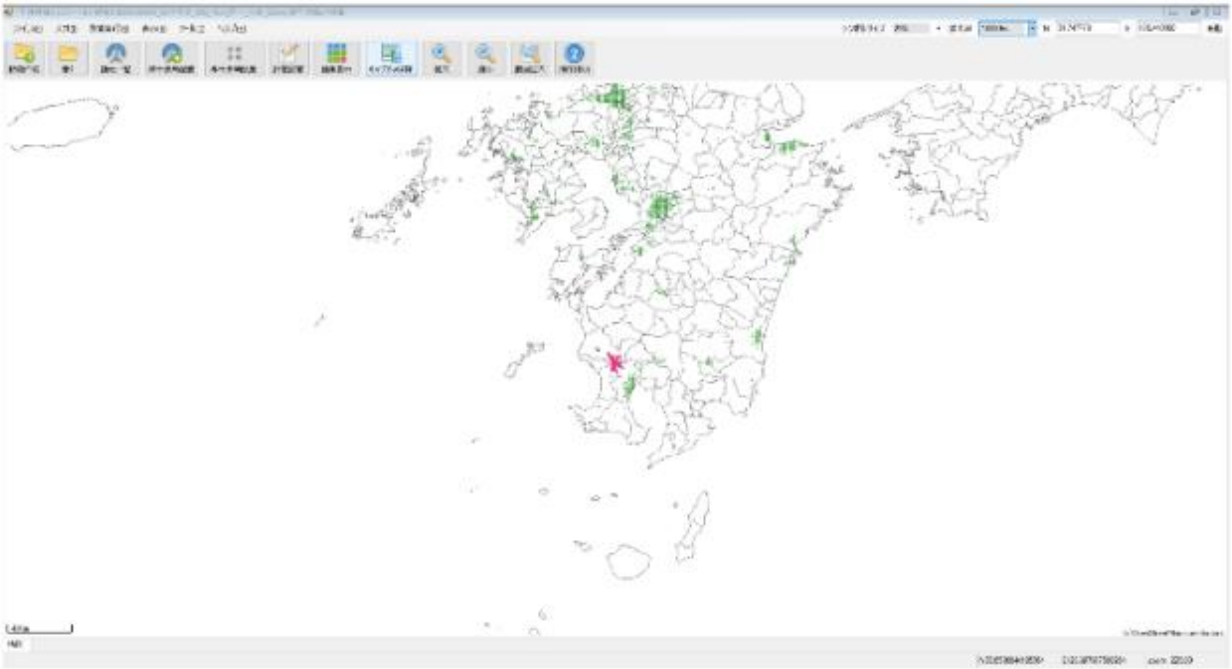

Figure A3-8 shows the results of evaluating the magnitude of the interference power to the RAS observatory from the individual BSs at each location depending on the distance from the RAS observatory. In this figure, a blue plot shows the magnitude of the interference power from each IMT BS, and the red horizontal line shows the threshold interference power (within the band) at the RAS observatory. The averaged antenna pattern of the IMT BS was used in evaluating interference power (see Fig. A3-1).

Figure A3-8 shows that the magnitude of the interference power from the IMT BSs satisfies the threshold interference power at the RAS observatory under the in-band interference condition if a separation distance of about 40 km or more is secured. In addition, under the condition of adjacent-band interference, the threshold interference power at the RAS observatory is satisfied if a separation distance of about 35 km or more is secured. Even under the above-mentioned conditions within the separation distance, threshold interference power at the RAS observatory may be satisfied in some cases depending on the location of the IMT BSs, the terrain existing on the propagation path to the RAS observatory, or the shielding condition from buildings.

FIGURE A3-8

Received interference power at the VERA Iriki station from IMT BSs

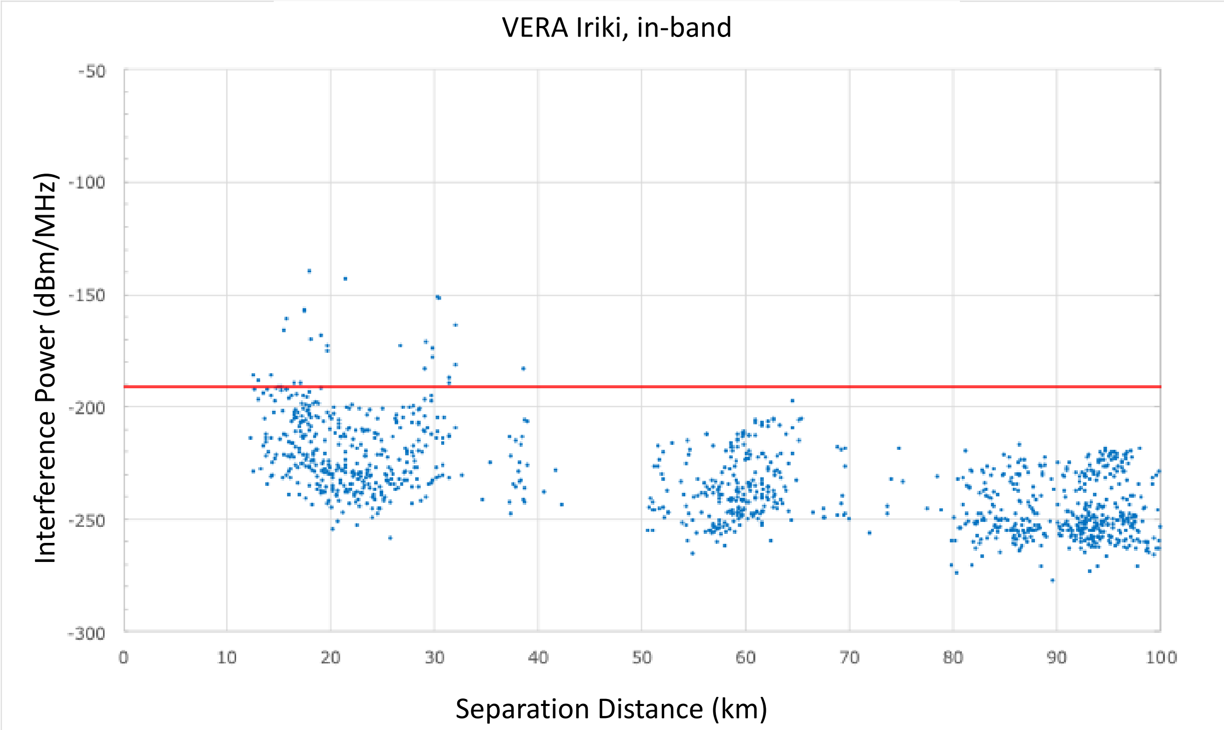

a) In-band interference

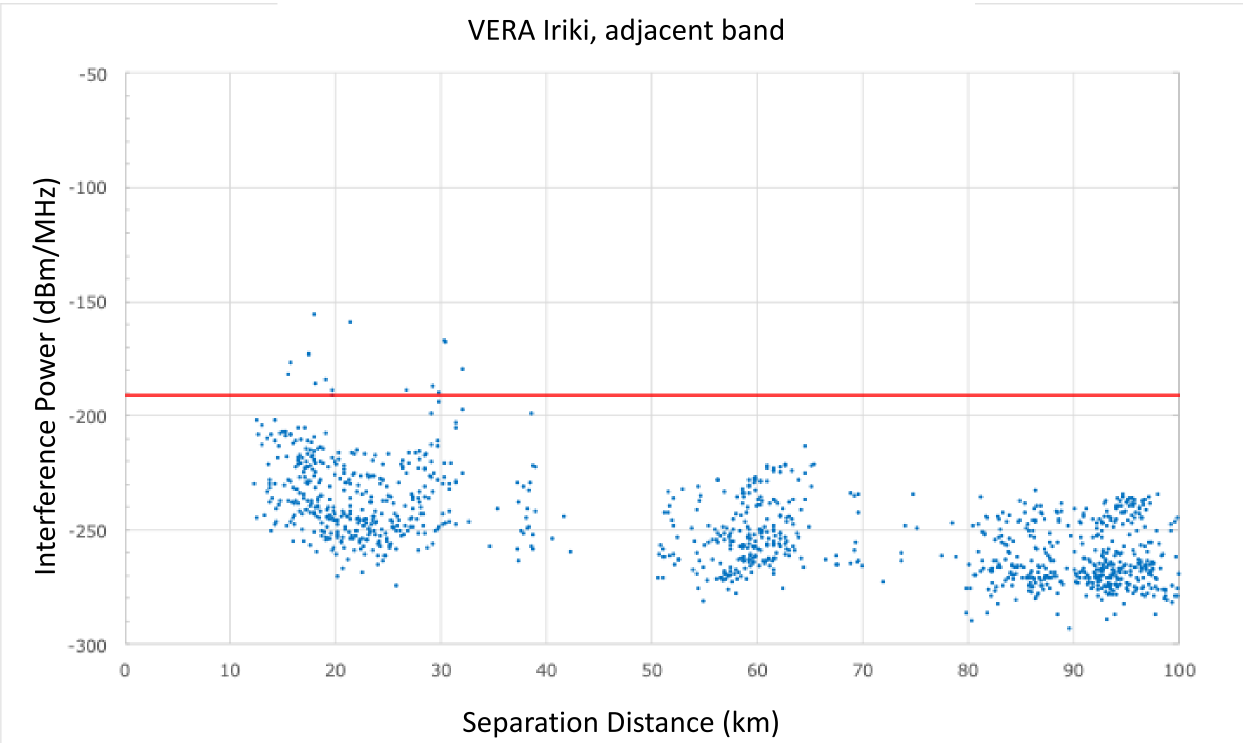

b) Adjacent-band interference

Table A3-7 shows the calculation results for the number of IMT BSs that can be installed when aggregate interference is taken into consideration. Threshold values of −201 dBm/MHz and −211 dBm/MHz were set for determining whether to install an IMT BS at each point, considering

6 009 points in the Kyushu area selected based on the daytime population. These threshold values are adopted as 10 dB and 20 dB, respectively, lower than the threshold interference power (i.e. the protection criterion) at the RAS observatory. The interference margin in this Table gives the difference between the cumulative interference power (aggregate interference power) from multiple IMT BSs, and the threshold interference power at the RAS observatory when the maximum installable number of IMT BSs are installed.

Table A3-7 shows that more than 5 000 IMT BSs satisfying the threshold interference power at the RAS observatory can be installed in the Kyushu area if the threshold value of the interference power that determines whether to install the BS is set appropriately.

TABLE A3-7

Maximum installable number of IMT BSs for the aggregate interference case

(a) In-band case		
Interference threshold value (dBm/MHz)	−201	−211
Maximum installable number of IMT BSs	5 192	4 944
Number of points where IMT BSs are not installable	319	567
Interference margin (dB)	6.5	14.9
(b) Adjacent-band case		
Maximum installable number of IMT BSs	5 372	5 264
Number of points where IMT BSs are not installable	139	247
Interference margin (dB)	9.0	18.2

A3.3 Summary of study

The study results on sharing and compatibility between RAS observatories and IMT BSs are summarized in Table A3-8.

TABLE A3-8

Summary of sharing and compatibility studies between RAS observatories and IMT BSs

In-band case	• Based on three case studies within Japan, a separation distance of 35-45 km is required for the IMT BSs to satisfy the threshold interference level for protecting the RAS observations; • For the aggregate interference case from multiple BSs, it is possible to deploy more than a few thousand BSs if the appropriate interference threshold for judging the deployment, which is lower than the value defined in Rec. ITU-R RA.769, is adopted while keeping the separation distance mentioned above.
Adjacent-band case	• Based on three case studies within Japan, a separation distance of 30-40 km is required for the IMT BSs to satisfy the threshold interference level for protecting the RAS observations; • For the aggregate interference case from multiple BSs, it is possible to deploy more than a few thousand BSs if the appropriate interference threshold for judging the deployment, which is lower than the value defined in Rec. ITU-R RA.769, is adopted while keeping the separation distance mentioned above.

It is noted that the IMT mobile stations transmit radio waves only under the condition that they can receive radio waves from an IMT BS. Therefore, the IMT mobile stations in the area where a BS is installed, under the condition that they can share frequencies with the RAS (e.g. the condition of securing the separation distance shown above), is considered to be able to share frequencies with the RAS observatory if the following characteristics of IMT mobile stations are satisfied: 1) the antenna height is low enough; 2) the transmission power is controlled; and 3) the number of stations that transmit radio waves at the same time is only a few per BS, and their frequency bands are different.

However, if the separation distance is short, there may be a case that no shielding can be obtained between the IMT mobile station in the IMT BS service area and the RAS observatory, even when it is judged that they can share frequencies by reducing interference power through shielding from buildings, etc. In such a case, careful examination is required to determine if sharing is feasible in order to avoid the risk that the RAS observatory could be affected by interference from the IMT mobile stations.

Annex 4

Sharing and compatibility studies for European radio observatories

A4.1 Introduction

In Europe, several major RAS facilities are equipped with state-of-the-art receivers to observe in the 42.5-43.5 GHz RAS band. To complement the generic (flat-terrain) sharing and compatibility studies in Annex 1, here site-specific single-interferer separation distances are derived, accounting for real terrain around the sites. In particular the 100-m radio telescope at Effelsberg is subject to quite good natural terrain shielding at these frequencies. The following RAS sites were considered: 100-m radio telescope at Effelsberg (DEU), Cambridge MERLIN telescope (UK), Noto 32-m (IT), Onsala 20-m (S), Sardinia Radio Telescope (IT), and Yebes 40-m (ESP).

A4.2 Study parameters

The study parameters are the same as in § A2.1. Results are provided for a typical value of the Recommendation ITU-R P.2108, § 3.2 clutter loss model, i.e. averaged over a uniform distribution of p_L values. Again, it must be noted, that the model in Recommendation ITU-R P.2108 is appropriate for urban and suburban land cover types and only if the IMT devices are below the rooftops of the housings. As in some countries, these conditions are not fulfilled when assignments are made, in the following the results for zero clutter loss values will also be provided for comparison.

A4.3 Singe-interferer scenario

The method to derive single-interferer separation distances for the in-band and spurious-domain cases is the same as in § A2.2. The only difference is that here the actual terrain heights around the sites of interest are considered in the application of the path propagation model (Recommendation ITU-R P.452). The results are shown in Figs A4-1 to A4-6 for maps of 150 km × 150 km size, and were only calculated for suburban open-space hotspots. These have somewhat higher antenna heights, but at the same time a larger down-tilt, such that the results are not significantly different from urban/suburban hotspots. Except for Jodrell Bank observatory, terrain height profiles are based on very precise Lidar measurements[4]. For Jodrell Bank, SRTM[5] data were used, as no Lidar data set was available at the time of this study.

The assumption was made that the antennas are tilted down and that the beam never points above the horizon. However, this restriction does not lead to significantly reduced coordination zone sizes, as Fig. A4-7 reveals, in which the resulting map is put side-by-side with a map calculated based on the maximum possible antenna gain. Only in very mountainous terrain it makes a difference, in more open terrain, the typical horizon elevation angles are too close to zero to have an impact. For the spurious case, the difference is not notable.

FIGURE A4-1

Single-interferer separation distances for the 100-m radio telescope at Effelsberg (Germany)

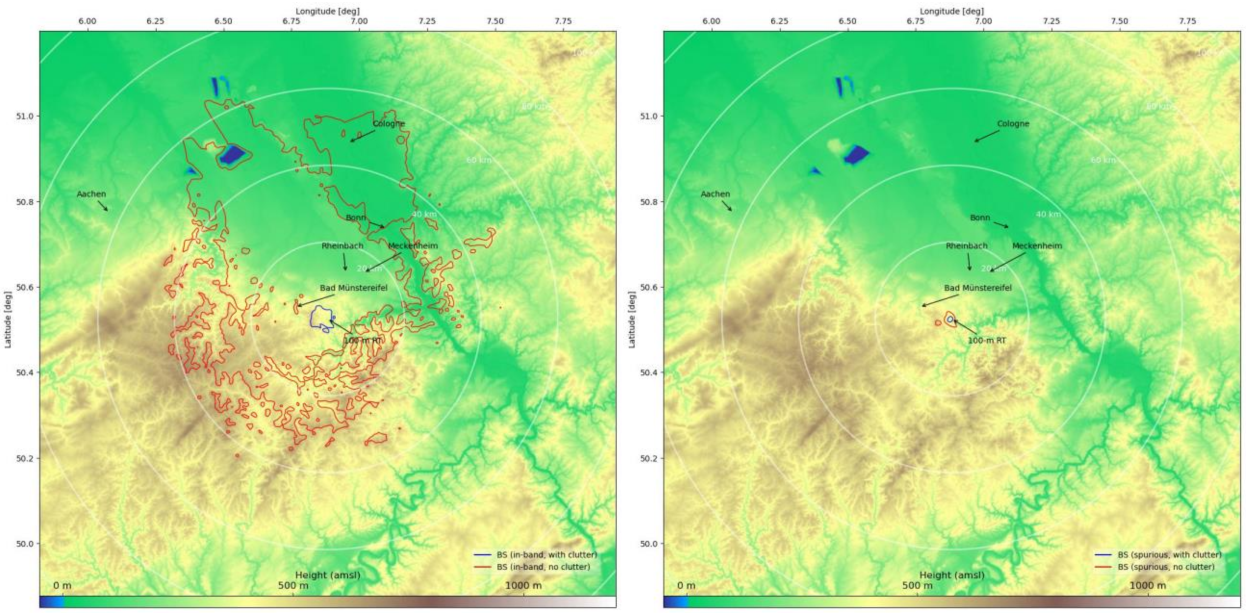

---

4 Terrain height data bases for the different RAS stations used in this Report, based on a compilation by Open Data Portal, Austria:

– Effelsberg, DEU: Land Nordrhein-Westfalen (2017), DTM 1 Meter & Landesamt für Vermessung und Geobasisinformation Rhineland-Palatinate: DTM 25 Meter (DGM25); License: Datenlizenz Deutschland Namensnennung 2.0.

– Noto, IT: Regione Siciliana: MDT 2012-2013 2x2 ETRS89 (= DTM 2 m).

– Onsala, S: Lantmäteriet (Swedish Land Survey): "Höjddata, grid 50+" DTM 50 Meter.

– SRT, IT: Regione Autonoma della Sardegna, Sardegna Geoportale: DTM 1 m and 10 m.

– Yebes, ESP: LiDAR-PNOA assigned by Instituto Geográfico Nacional (IGN): DTM02/05.

5 T. G. Farr, P. A. Rosen, E. Caro, R. Crippen, R. Duren, S. Hensley, M. Kobrick, M. Paller, E. Rodriguez, L. Roth, D. Seal, S. Shaffer, J. Shimada, J. Umland, M. Werner, M. Oskin, D. Burbank and D. Alsdorf, *The Shuttle Radar Topography Mission*; Reviews of Geophysics, vol. 45, 2007.

FIGURE A4-2

Single-interferer separation distances for the Cambridge MERLIN telescope (UK)

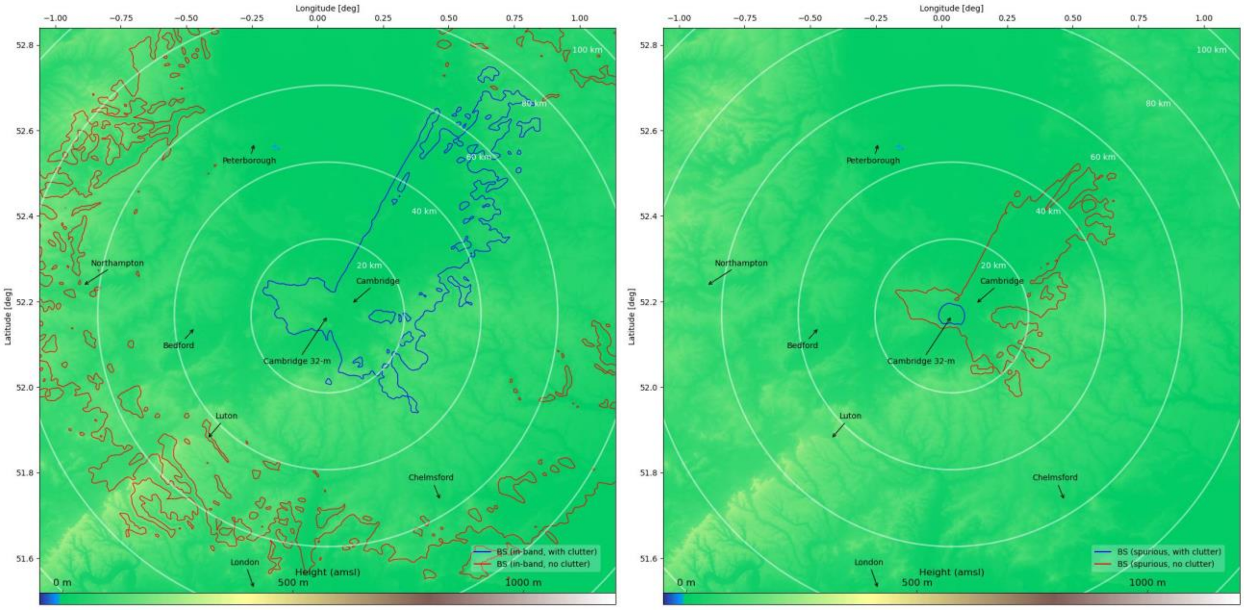

FIGURE A4-3

Single-interferer separation distances for the Noto (IT)

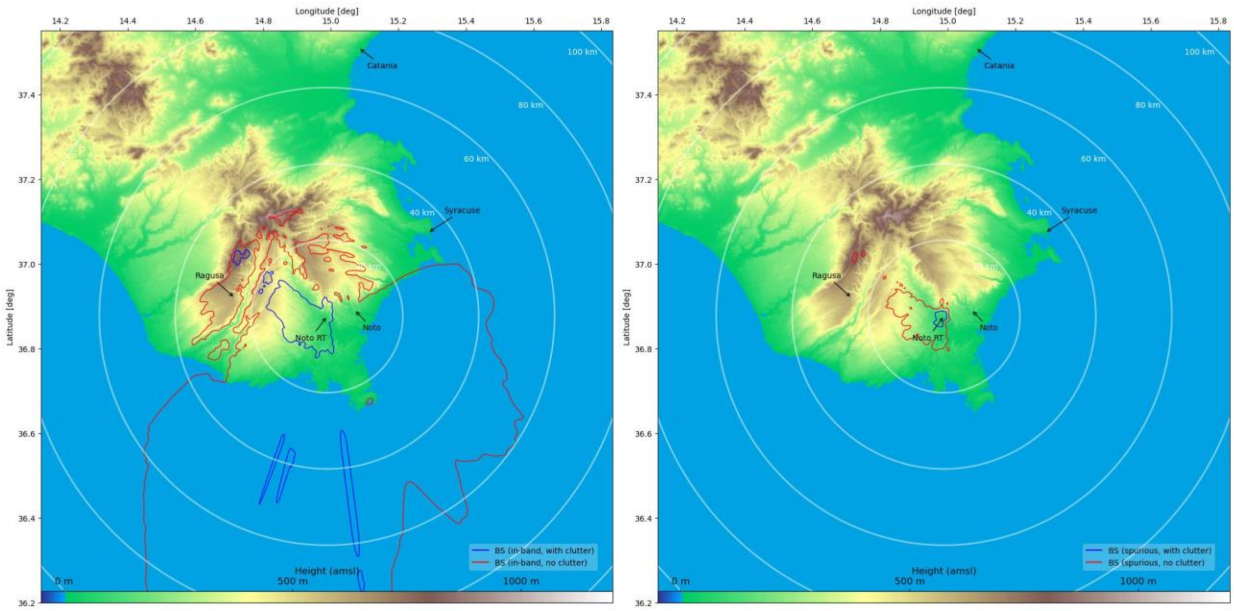

FIGURE A4-4

Single-interferer separation distances for the Onsala 20-m (S)

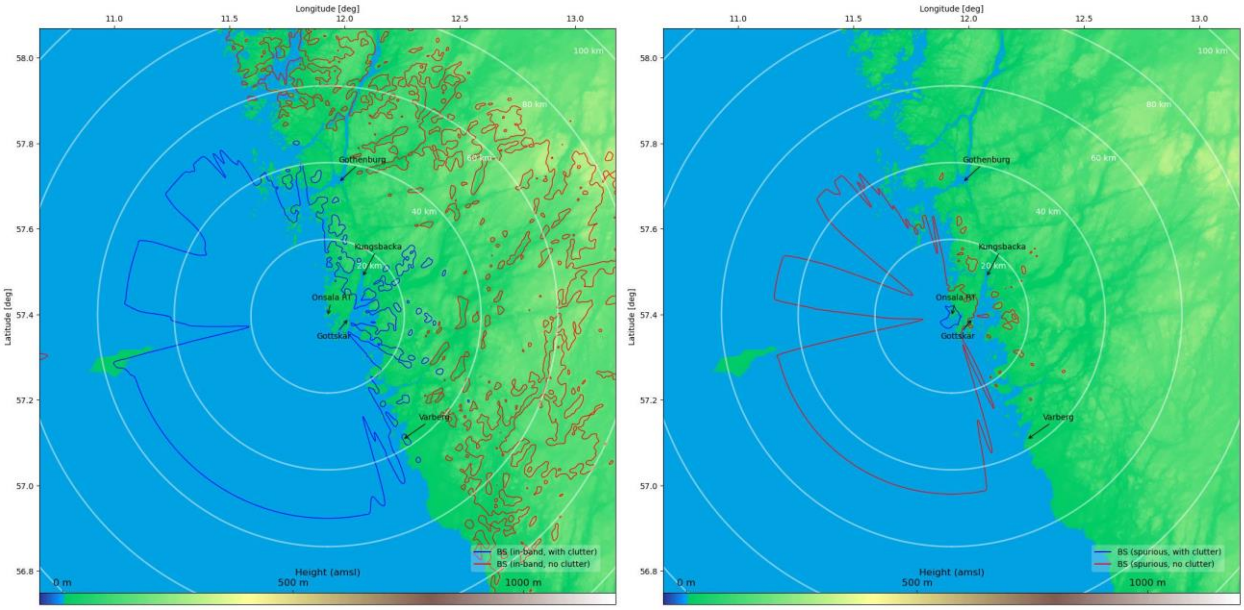

FIGURE A4-5

Single-interferer separation distances for the Sardinia Radio Telescope (Italy)

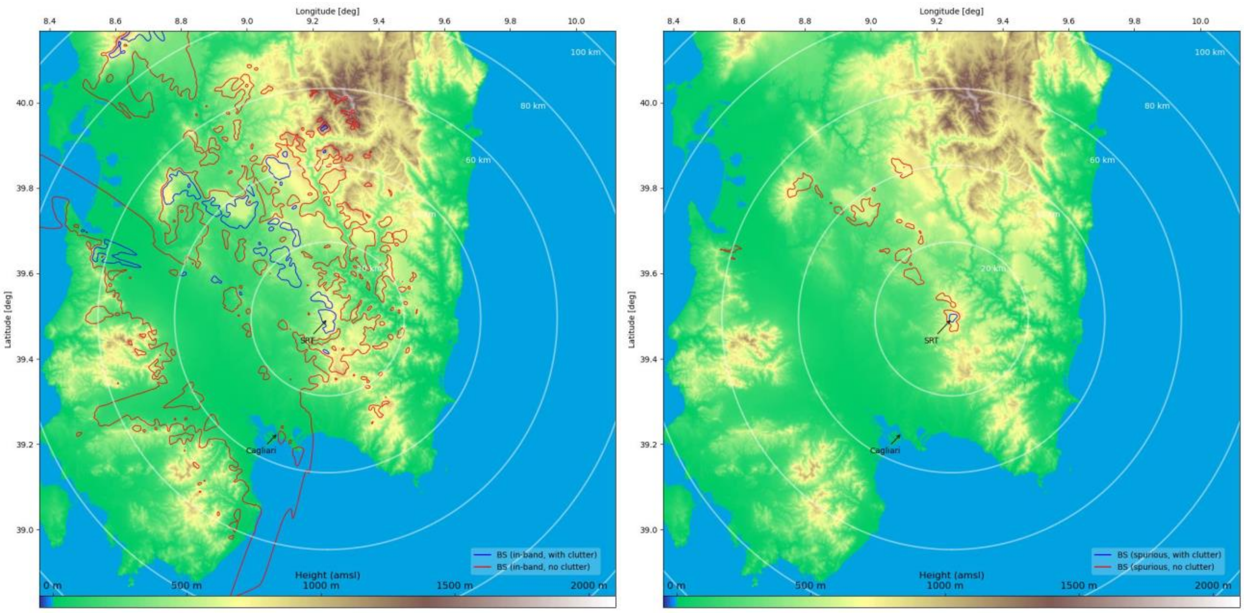

FIGURE A4-6

Single-interferer separation distances for the Yebes 40-m radio telescope (Spain)

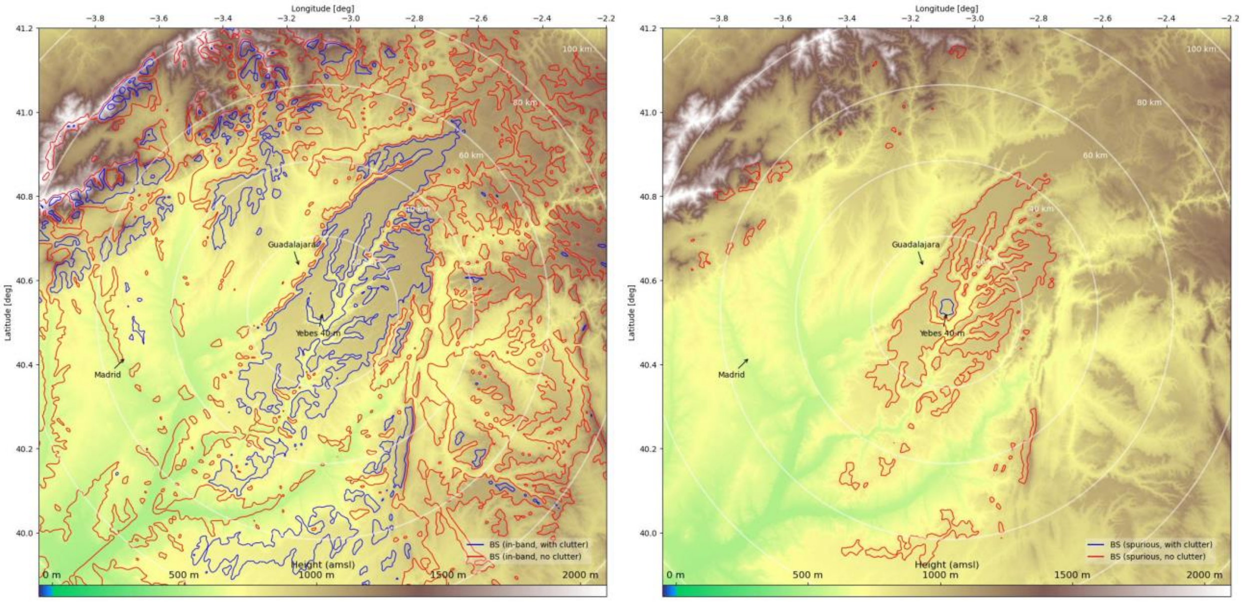

FIGURE A4-7

Comparison between max-gain case (left) and below-the-horizon restriction for the BS beams (right) based on the example of the 100-m radio telescope at Effelsberg (Germany)

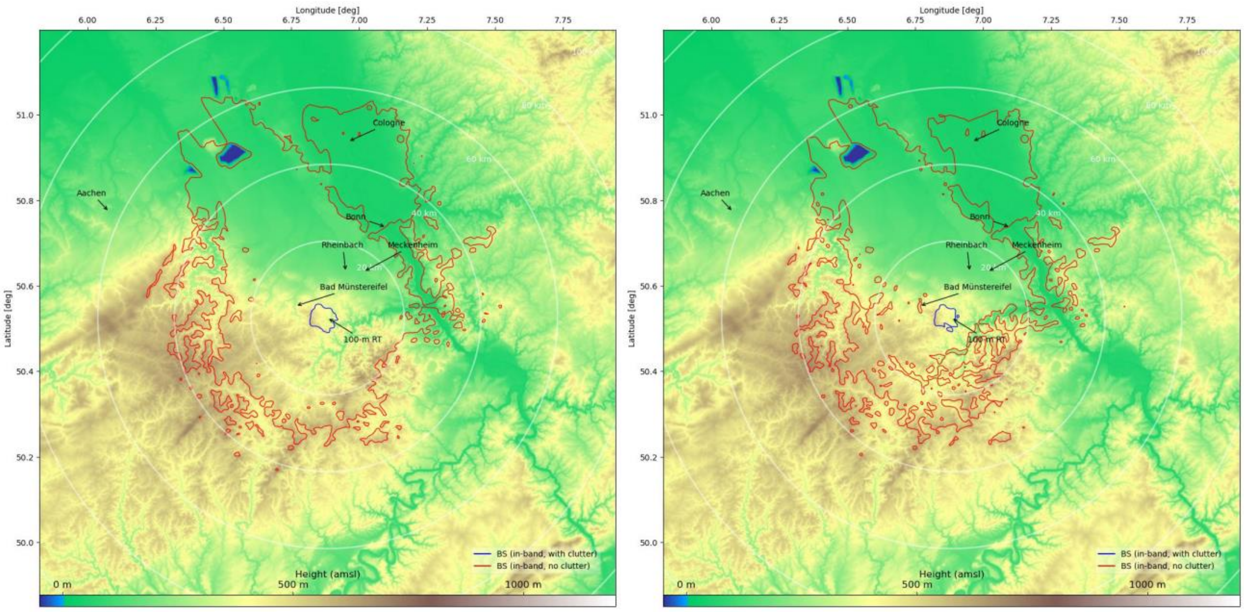

A4.4 Summary

The results indicate that in the single-interferer worst-case scenario separation distances of up to 60-80 km could be required in the sharing scenario, or even more if the IMT BS are not subject to clutter losses. For the spurious domain case, when IMT is active in the adjacent band (with a sufficient guard band) the situation is more relaxed. Only the immediate vicinity (<5 km) of the RAS stations needs to be controlled. However, without the substantial shielding by clutter (according to the model in P.2108), the separation distances can also become significant, in the order of up to 60-80 km. An exception is the 100-m telescope at Effelsberg in Germany, for which natural terrain shielding is very efficient. As long as clutter applies, separation distances are less than 10 km in all cases.

The results demonstrate very well, how fundamental the assumed clutter losses are for the sharing and compatibility between IMT and RAS. Co-existence is well possible, but IMT BS must not be put at elevated heights, i.e. above the local roof-tops (assuming that deployment is in urban or suburban area only). Otherwise, IMT devices could cause interference to the RAS over significant distances. Of course, other mitigation measures could be applied to counteract missing clutter, e.g. the IMT antennas could be directed away from the RAS station. The restriction that base-station beams should never be pointed to above the horizon has not a large effect and cannot be considered as an important mitigation measure in many practical cases.